

1 **Responses to Reviewer's Comments to**

2 Zhang et al., "*Fossil vs. non-fossil sources of fine carbonaceous aerosols in four Chinese*
3 *cities during the extreme winter haze episode in 2013*"

4

5 We thank the reviewers for their comments on our paper. To guide the review process we
6 have copied the reviewer comments in black color font. Our responses are in blue font. We
7 have responded to all the referee comments and done the modifications accordingly.

8

9 Anonymous Referee #1

10 General comments:

11 This manuscript describes radiocarbon source apportionment of organic aerosols during
12 winter-time smog episodes in China. Air quality is a big concern in Chinese cities and
13 especially the sources and formation mechanisms of organic aerosol are still un-certain. Using
14 radiocarbon for source apportionment of organic aerosols is a very useful method, because,
15 unlike tracer ratios, the ^{14}C signature of the sources is not changed by chemical
16 transformations in the atmosphere.

17 The methods and results are described clearly. The results are very relevant, showing that
18 winter haze episodes do not necessarily result from an increase of specific fossil or non-fossil
19 sources, but from an accumulation of pollutants accompanied by strong formation of
20 secondary organic aerosol.

21 Given these results, the manuscript could be made significantly stronger, if the authors
22 would additionally investigate meteorological conditions and air mass histories and their
23 potential role in the pollution episodes. If the conditions could be identified that favor the
24 accumulation of pollutant and secondary organic aerosol formation, this would give important
25 insight into the pollution episodes.

26 However, the presented results are sufficiently interesting and important to be published
27 and therefore I recommend acceptance with minor revisions, detailed below.

28 Reply: We thank the reviewer for the nice summary of our paper and the positive
29 comments. In the following we will respond to each comment listed below separately. The
30 primary objective is to study fossil versus non-fossil contribution to both the OC and EC
31 during the moderately polluted days and heavily polluted days. As a result, we did not include
32 intensive discussion on how meteorological conditions affect PM and SOA formation in
33 current study. Actually, this kind of studies has already been reported in several other studies
34 (Wehner et al., 2008; Zhang et al., 2014). In the revised MS, we add following sentence in
35 Sec 3.1: "The higher PM_{2.5} mass, OC and EC observed during the polluted period was
36 characterized by low wind speed but not significantly sensitive by the temperature and

1 relative humidity.” Concerning air mass back trajectory, we did not find any significant
2 dependence between PM2.5 (OC, EC) and air mass origins (see the response and Figure R2
3 below). Therefore, we decided not include air mass back trajectory analysis in this study.

4 Specific comments:

5 p26264, line 10ff: Is the uncertainty for $f_m(\text{OC})$ based on the reproducibility of the
6 sunset OC/EC measurements and the uncertainties of the fraction modern? If, yes, please state
7 so explicitly. In principle the uncertainty of EC-OC determination is much larger than the
8 reproducibility derived from using one particular protocol. Inter-laboratory comparisons using
9 different protocols for EC-OC determination show much larger uncertainties, on the order of
10 30% for EC. Please discuss this and estimate a resulting uncertainty for $f_m(\text{OC})$.

11 Reply: the uncertainty for $f_m(\text{OC})$ (8%) was obtained from an error propagation and
12 include all the individual uncertainties of the $f_m(\text{TC})$ (2%), $f_m(\text{EC})$ (5%), TC (8%) and EC
13 (25%). The sentence is changed as “The uncertainty of $f_m(\text{OC})$ estimated by this approach is
14 on average 8% obtained from an error propagation and include all the individual uncertainties
15 of the $f_m(\text{TC})$ (2%), $f_m(\text{EC})$ (5%), TC (8%) and EC (25%).” We would also like to emphasize
16 that the variability of EC concentrations between different protocols is substantially reduced,
17 if water-extracted filters are used (see Zhang et al., 2012 in MS).

18 p26272, line 7: What are the uncertainties given here (standard deviation, standard error
19 of the mean, propagated experimental uncertainties)?

20 Reply: it is standard deviation. The sentence is changed as “OCf contributions (mean±
21 standard deviation) to total OC were $37 \pm 3 \%$...”

22 p26272, line 11: You mean the variability between different cities? Because within each
23 city the fraction of OCf in OC still seems relatively constant

24 Reply: yes. The sentence is changed as “The large variability of the fraction of OCf to
25 total OC among the different cities...”

26 p26273, line 11: Please give a reference for the lev-to-K ratio in hardwood burning.

27 Reply: the reference is now added.

28 p26273, line 25: Please note that in the corresponding figure, $\text{OC}_{\text{other,nf}}$ is called OC_{bio}

29 Reply: the figure is now changed.

30 p26273, line 27ff: In this sentence it is already assumed that $\text{OC}_{\text{other,nf}}$ is mainly
31 secondary aerosol. This is discussed in more detail later. Please state this more clearly here, or
32 maybe already on page 26267, line 5ff.

33 Reply: The sentences are changed as “Despite a large spread of $\text{OC}_{\text{sec,f}}$ and $\text{OC}_{\text{other,nf}}$, the
34 data conclusively shows that both contributions were always larger on the heavily than on the
35 moderately polluted days, highlighting the importance of fossil-derived SOC formation and
36 other non-fossil emissions excluding primary biomass burning sources. The increased
37 $\text{OC}_{\text{other,nf}}$ is likely due to enhanced SOC formation from biomass burning and other non-fossil

1 sources (see Sec. 3.3).”

2 p26274, line 22ff: Here you state very generally that SOC from non-fossil sources is
3 mainly from biomass burning. However, this need not necessarily be true for SH and GZ,
4 where temperatures during this time period are well above 0 degrees.

5 Reply: yes, the biogenic SOC could not be excluded for SH and GZ. The sentence is
6 changed as “The dominating contribution of $OC_{\text{other, nf}}$ is likely due to the increase of SOC
7 formation from non-fossil sources mainly from biomass-burning emissions, although
8 biogenic-derived SOC could not be excluded for SH and GZ where temperatures during the
9 sampling period are above 0 degrees. ”

10 p26275, line 9: Do you mean here the fossil contribution to primary aerosol?

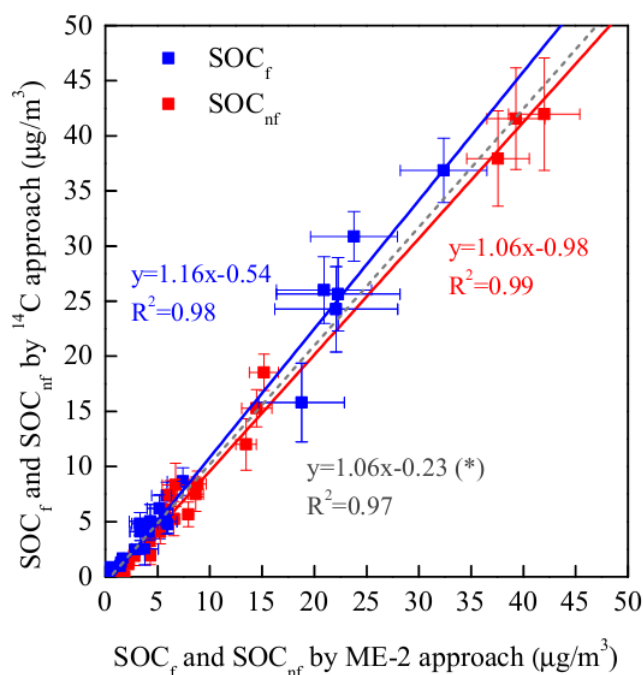
11 Reply: “fossil contribution” here means “fossil contribution to TC” which is now
12 clarified.

13 P26276, line 10: Given that Huang et al., 2014 reached similar conclusions for total
14 PM_{2.5}, I think comparing the results and conclusions between these two studies, should go
15 further than just comparison of the source apportionment methods. Please compare the results
16 of this study to Huang et al., 2014 in more detail.

17 Reply: the primary objective of our study is to investigate sources and formation
18 mechanisms of fine carbonaceous aerosols. The comparison between this study and Huang et
19 al., 2014 is to evaluate the LHS model performance used in this study (see Sec2.5). We
20 believe that both studies have already given sufficient but different information, so further
21 comparison between 2 studies is not necessary.

22 P26276, line 25: A slope of 1.13 is usually not called a 13% offset. More often, the
23 intercept of the regression line is called ‘offset’. In general, it is better not to force the
24 regression line through 0, because the intercept also contains information. Please change this.

25 Reply: The term “offset” was changed to “deviation” in the text. As the intercept is
26 statistically insignificant (see below in Fig. R1), we remained the figure as it was and added
27 the sentence to the caption: “Note that the intercepts are insignificant for all three cases.”



1
2
3
4
5
6
7
8
9
10
11
12
13
14
15
16
17
18
19
20
21

Figure R1: Figure 7 with intercepts for the three cases. All of which are statistically insignificant so that we omit to show them in the manuscript.

Figure 5: The labeling in this Figure is much too small. I had to use 400% magnification to read the subscripts. Maybe using on general legend for all the figures (e.g. on the top) would be a solution:

Reply: the figure is now changed according to the reviewer's comment.

Anonymous Referee #2

This paper describes a source apportionment of the carbonaceous component of 24h samples of PM2.5 collected in four major cities in China in January 2013, when total PM2.5 concentrations reached very high levels (up to 100s g m-3). The source apportionment is principally based on the proportion fossil/non-fossil carbon in the TC, and in the OC and EC fractions, as determined from accelerator mass spectrometry (AMS) measurements of the amount of the radiocarbon isotope, 14C, in the carbon. These data were supplemented by measurements of the levoglucosan, mannosan and water-soluble K+ concentrations in the PM2.5 which provide additional information for the source apportionment of biomass burning.

Both the analytical and data-interpretation methodologies for this study follow very closely that of a number of previous studies, particularly in Europe, undertaking similar

1 source apportionment of the carbonaceous aerosol. This has the advantage of use of
2 methodology that has already been through the peer-reviewed literature. The novelty here is
3 its application to PM2.5 samples in very large Chinese cities that have experienced PM2.5
4 levels up to an order of magnitude greater than in many European urban locations. Poor air
5 quality in China is clearly a major cause for concern and it is important for all, particularly
6 policy-makers, to have insight into the constituent components and sources of the PM2.5.

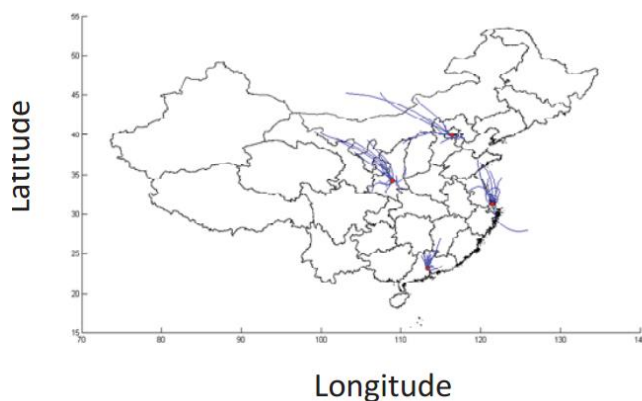
7 Key results from this study include the finding of substantial non-fossil contribution to
8 OC (in common with similar studies globally) and the inference that a substantial fraction of
9 this non-fossil OC is primary rather than secondary in nature. The authors also compared their
10 source apportionments between the most heavily-polluted days and moderately polluted days
11 and noted that despite the increase in absolute masses the proportion of secondary was even
12 slightly higher.

13 The paper describes thorough experimental procedures and appropriate data analysis
14 methodologies. The writing is generally fluent, although occasional grammar and comma
15 punctuation usage requires amendments. I have a couple of points regarding scientific
16 interpretation, and the remaining points are largely concerned with presentation. I recommend
17 this paper as suitable for publication in ACP following attention to these issues and any other
18 relevant issues raised by other reviewers.

19 Reply: we thank the reviewer for the nice summary of our paper and the positive
20 comments. In the following we will respond to each comment listed below separately.

21 (1) The authors could likely gain some greater insight into the origin of their various
22 carbon fractions by undertaking an air-mass back-trajectory investigation for the days of their
23 samples, particularly through a comparison of the high-pollution vs. moderate-pollution days.

24 Reply: the carbon fraction is not dependent on air mass origins. The air mass back
25 trajectory analysis (see Figure R2 below) shows the prevailing air masses are generally from
26 the north during our measurement period which has already been reported by Huang et al.
27 (2014). As a result, it is not included in the current study.



1
2
3
4
5
6
7
8
9
10
11
12
13
14
15
16
17
18
19
20
21
22
23
24
25
26
27

Figure R2: Air mass back trajectories of air arriving the measurement sites on each measurement day, calculated using the NOAA HYSPLIT model (Huang et al., 2014)

(2) The description and nomenclature of the divisors used in Equations (3) and (5) was not immediately clear to me, i.e. the terms $f_M(bb)$ and $f_M(nf)$ in the two equations respectively. I interpret these terms as being the values used to correct the $f_M(EC)$ and $f_M(OC)$ values to yield a fraction contemporary carbon in EC and OC, rather than the fraction modern carbon in EC and OC. In my opinion, the terminology $f_M(bb)$, and the phrase “a ^{14}C reference value for biomass burning” do not make it clear that the reference value is the percent modern in EC emitted from burning contemporary carbon-containing fuel. Likewise, for lack of clarity in Equation (5). The application of these terms does not become clearer until the text in point #1 on P26267.

Reply: To make the Equation (3) clearer, the sentence is changed as “ EC_{bb} is calculated from the EC mass concentration, $f_M(EC)$ and a reference value of biomass-burning EC (i.e. fraction of modern in EC emitted from biomass burning sources, $f_M(bb)$)”. To make the Equation (5) clearer, the sentence is changed as “Analogously, OC is divided into two sub-fractions, OC from fossil fuel (OC_f) and non-fossil emissions (OC_{nf}). To account for the thermonuclear weapon tests of the late 1950s and early 1960s, OC_{nf} is calculated from the OC mass concentration, $f_M(OC)$ and a ^{14}C reference value of non-fossil emissions (i.e. fraction of modern in OC emitted from non-fossil sources, $f_M(nf)$).”

Technical corrections:

Abstract: State the collection duration of each PM2.5 sample (24 h).

Reply: it is added.

Abstract: State the number of samples analysed for ^{14}C , i.e. the number of sample values that underpin the mean and standard deviation of source apportionment proportions presented in the abstract.

Reply: it is added.

1 P26259, L6: Rephrase end of the sentence as “...was conducted at the four major cities of
2 Xian, Beijing, Shanghai and Guangzhou.” (The fact that the study was conducted in several
3 large cities in China has already been stated in the previous sentence.)

4 Reply: it is corrected.

5 P26259, L7. Delete “An effective” and start the sentence directly as “Statistical analysis
6 of:” Remove the words “An effective” from in front of similar phrasing elsewhere in the
7 paper where the Latin Hypercube technique is mentioned; it is a redundant adjective.

8 Reply: it is corrected.

9 P26259, L11: Rewrite as “across all sites.”

10 Reply: this is corrected.

11 P26259, L19: Delete “rather”.

12 Reply: this is corrected.

13 P26260, L1: Delete both the two commas.

14 Reply: this is corrected.

15 P26261, L9: Delete comma.

16 Reply: this is corrected.

17 P2621, L22: Please provide a quantitative indication of what is meant by “extremely high
18 concentrations of PM2.5”

19 Reply: It is changed as “During January 2013, the severe problem of air pollution in
20 China became a worldwide concern, as extremely high concentrations of 24-h PM2.5 (i.e.
21 often >100 μm^3) were reported in several large cities affecting ~1.3 million km^2 and ~800
22 million people.”

23 P26263, L4: “Six filters were selected:”

24 Reply: this is corrected.

25 P26265, L12: Sort out the formatting of the citation in this sentence.

26 Reply: this is corrected.

27 P26267, L21: Insert “for” to read “To correct for the:”

28 Reply: this is corrected.

29 P26271, L16: Correct the sentence containing the phrase “...with an equally
30 enhancement:” which doesn’t make grammatical sense.

31 Reply: the sentence is changed as “This finding suggests that the increase of EC_f and
32 EC_{bb} emissions in the three cities on the heavily polluted days is likely due to an equal
33 enhancement of fossil fuel and biomass-burning combustion emissions and the accumulation
34 of these particulate pollutants.”

35 P26272, L13: Should this read the “ratio of EC_f to OCP ”?

36 Reply: this is corrected.

37 P26273, L6: Insert comma after “marker”

1 Reply: this is corrected.

2 P26273, L7: Insert comma after “)”

3 Reply: this is corrected.

4 P26277, LL6&&: Provide a definition here of the two acronyms MPD and HPD.

5 Reply: the sentences are changed as: “Furthermore, it decreases the $OC_{sec,f}$ -to- $OC_{pri,f}$ ratio
6 of Beijing from 2.7 and 5.9 to 1.2 and 2.9 for the moderately and heavily polluted days,
7 respectively. As a consequence, these values become better comparable with those of the
8 other cities, but still underline the importance of secondary aerosol formation during the
9 heavily polluted days.”

10 P26295: Delete the word “below” from the last line of the caption of Figure 6.

11 Reply: this is corrected.

12 Supplementary information, caption to Table S1: Should read “The sampling dates for
13 the:..”

14 Reply: this is corrected.

15 Anonymous Referee #3

16 The manuscript presents comprehensive and well-established methodology to reveal the
17 sources of fine carbonaceous aerosols in China under conditions of heavy pollution episodes.
18 The approach taken by the authors is not particularly innovative, it is put together from
19 previous works, many of which are linked to the authors themselves. Nevertheless, it is worth
20 publication since it deals with pollution levels not frequently encountered in other parts of the
21 world, and applies methods that are adequate, up-to-date and well-proven in similar studies.
22 However, I have two major points that need to be addressed before publication in ACP

23 Reply: we thank the reviewer for the nice summary of our paper and the positive
24 comments. In the following we will respond to each comment listed below separately.

25 1) On Page 26266, as part of their own innovation, the authors introduce a p factor that is
26 intended to split OC/EC primary emission factor between coal combustion and vehicular
27 emission. p is simply defined as a percentage of coal combustion within total fossil fuel
28 emission in China. Since the focus of this study is exclusively fine particulates, and coal
29 combustion and tailpipe emission is well-known to produce fundamentally different size
30 distributions, the use of this overly simplified p factor cannot be justified. This should either
31 be omitted or estimated on the basis of relevant studies that take into account the size-
32 resolved emission factors from both coal combustion and vehicular emission.

33 Reply: we agreed that the size distribution may differ in particles emitted from coal and
34 tailpipe emission. However, it should be noted that the size of particles emitted from coal and
35 tailpipe are mostly smaller than 2.5 μm (the particle size used in this study) (Huang et al.,
36 2006; Zhang et al., 2012). As a result, the size distribution would not affect our results if we
37 did not study fossil and non-fossil carbon in size-resolved particles (i.e. from 0.056 μm to 10

1 μm). In fact, a very large range of p (0-0.7) instead of simply p value was used in the study. In
2 addition, when increasing the p value (i.e. from 0.35 to 0.70 for central p value) for Beijing,
3 we found ECf, ECbb, OCbb and OCother, nf are independent of the choice of the p value (see
4 Table S2 and Fig. S1), although the contribution of SOCF was decreased, but still underlining
5 the importance of fossil-derived SOC. Moreover, the comparison of our study and Huang et al
6 (2014) confirmed that our source apportionment model and input parameters were justified.

7 2) My other major concern is related to the assumption that OCsecondary becomes
8 relatively more important in times of high levels of air pollutions. This issue is dis-cussed in
9 details in many previous source apportionment papers, and is partly related to nomenclature.
10 Can we consider enhanced particle-phase partitioning (condensation) of semi-volatile organic
11 compounds at colder temperatures simply as an increase in secondary organic aerosol (SOA)?
12 Traditional perception of SOA generally implies some photochemical transformations prior to
13 aerosol partitioning, which may not be the case here, at least not for the entire mass increment
14 that is declared to be OC-secondary. In my opinion, part of this apparent SOA is not SOA if
15 we strictly follow the definitions of atmospheric chemistry. However, the methodology
16 applied by the authors does not allow distinction to be made between simple condensation
17 and photochemical transformations. Thus, at least a critical discussion of the issue needs to be
18 added to the manuscript.

19 Reply: we agree that the condensation of semi-volatile organic compounds at colder
20 temperatures may contribute to the explained SOA in source apportionment study. However,
21 this contribution is very small compared to the real SOA enhancement because the
22 temperatures during the heavily polluted days were not significant lower than those found on
23 other days. So we do not believe that the increased SOA measured by our model is due to
24 condensation of semi-volatile organic compounds. The condensation of semi-volatile organic
25 aerosol generally may contribute with some extent to the measured SOA in winter but the
26 increased SOA between the moderately and heavily polluted days is largely due to enhanced
27 SOA formation. To make it clearer, the statement is added in Sec 3.3.1 "It should be also
28 noted that the condensation of semi-volatile organic aerosols generally may contribute to
29 some extent to the measured SOA in winter due to the colder temperature in the northern sites
30 such as Beijing and Xian. However, the increased SOA between the MPD and HPD measured
31 by the current method is mostly if not exclusively due to enhanced SOA formation since the
32 temperatures during the moderately and heavily polluted days were not significantly
33 different."

34
35 References:

36 Huang, X. F., Yu, J. Z., He, L. Y., and Hu, M.: Size distribution characteristics of elemental
37 carbon emitted from Chinese vehicles: results of a tunnel study and atmospheric

- 1 implications, *Environ. Sci. Technol.*, 40, 5355-5360, 2006.
- 2 Wehner, B., Birmili, W., Ditas, F., Wu, Z., Hu, M., Liu, X., Mao, J., Sugimoto, N., and
3 Wiedensohler, A.: Relationships between submicrometer particulate air pollution and
4 air mass history in Beijing, China, 2004–2006, *Atmos. Chem. Phys.*, 8, 6155-6168,
5 2008.
- 6 Zhang, H., Wang, S., Hao, J., Wan, L., Jiang, J., Zhang, M., Mestl, H. E. S., Alnes, L. W. H.,
7 Aunan, K., and Mellouki, A. W.: Chemical and size characterization of particles
8 emitted from the burning of coal and wood in rural households in Guizhou, China,
9 *Atmos. Environ.*, 51, 94-99, 2012.
- 10 Zhang, R., Li, Q., and Zhang, R.: Meteorological conditions for the persistent severe fog and
11 haze event over eastern China in January 2013, *SCIENCE CHINA Earth Sciences*,
12 57, 26-35, 2014.

1 **Fossil vs. non-fossil sources of fine carbonaceous**
2 **aerosols in four Chinese cities during the extreme**
3 **winter haze episode in 2013**

4
5 **Yan-Lin Zhang^{1,2,3,4,*}, Ru-Jin Huang², Imad El Haddad², Kin-Fai Ho^{5,6}, Jun-Ji**
6 **Cao⁶, Yongming Han⁶, Peter Zotter², Carlo Bozzetti², Kaspar R. Daellenbach²,**
7 **Francesco Canonaco², Jay G. Slowik², Gary Salazar^{1,3}, Margit Schwikowski^{2,3},**
8 **Jürgen Schnelle-Kreis⁷, Gülcin Abbaszade⁷, Ralf Zimmermann^{7,8}, Urs**
9 **Baltensperger², Andr  S.H. Pr  v  t², S  nke Szidat^{1,3,*}**

10 ¹Department of Chemistry and Biochemistry, University of Bern, Freiestrasse 3, 3012 Bern,
11 Switzerland

12 ²Paul Scherrer Institute (PSI), Villigen, 5232 Villigen-PSI, Switzerland

13 ³Oeschger Centre for Climate Change Research, University of Bern, 3012 Bern, Switzerland

14 ⁴Yale-NUIST Center on Atmospheric Environment, Nanjing University of Information
15 Science and Technology, Nanjing, Jiangsu, China

16 ⁵School of Public Health and Primary Care, The Chinese University of Hong Kong, Hong
17 Kong, China

18 ⁶Key Lab of Aerosol Science & Technology, SKLLQG, Institute of Earth Environment,
19 Chinese Academy of Sciences, Xi'an, 710075, China

20 ⁷Helmholtz Zentrum M  nchen, German Research Center for Environmental Health (GmbH),
21 Joint Mass Spectrometry Centre, Cooperation Group Comprehensive Molecular Analytics
22 and Helmholtz Virtual Institute of Complex Molecular Systems in Environmental Health —
23 Aerosol and Health (HICE), 85764 Neuherberg, Germany.

24 ⁸University of Rostock, Joint Mass Spectrometry Centre, Institute of Chemistry – Chair of
25 Analytical Chemistry, 18015 Rostock, Germany

26
27 *Correspondence to drvanlinzhang@gmail.com (Y. L. Zhang); szidat@dcb.unibe.ch (S.
28 Szidat)

29 Abstract

30 During winter 2013, extremely high concentrations (i.e. 4-20 times higher than the World
31 Health Organization guideline) of PM_{2.5} (particulate matter with an aerodynamic diameter <2.5
32 μm) ~~mass concentrations (24 hour samples) were reported found in four major cities in China~~
33 ~~including Xian, Beijing, Shanghai and Guangzhou several large cities in China. In this work,~~
34 ~~source apportionment of fine carbonaceous aerosols during this haze episode was conducted at~~
35 ~~four major cities in China including Xian, Beijing, Shanghai and Guangzhou. An effective~~
36 ~~statistical-Statistical~~ analysis of a combined dataset from elemental carbon (EC) and organic
37 carbon (OC), ¹⁴C and biomass-burning marker measurements using Latin-hypercube sampling
38 allowed a quantitative source apportionment of carbonaceous aerosols. ~~Based on ¹⁴C~~
39 ~~measurement in EC fraction (6 samples each city), We-we~~ found that fossil emissions from coal
40 combustion and vehicle exhaust dominated EC with a mean contribution of 75±8% ~~at-across~~ all
41 sites. The remaining 25±8% was exclusively attributed to biomass combustion, consistent with
42 the measurements of biomass-burning markers such as anhydrosugars (levoglucosan and
43 mannosan) and water-soluble potassium (K⁺). With a combination of the levoglucosan-to-
44 mannosan and levoglucosan-to-K⁺ ratios, the major source of biomass burning in winter in China
45 is suggested to be combustion of crop residues. The contribution of fossil sources to OC was
46 highest in Beijing (58±5%) and decreased from Shanghai (49±2%) to Xian (38±3%) and
47 Guangzhou (35±7%). Generally, a larger fraction of fossil OC was ~~rather~~ from secondary origins
48 than primary sources for all sites. Non-fossil sources accounted on average for 55±10% and
49 48±9% of OC and TC, respectively, which suggests that non-fossil emissions were very important
50 contributors of urban carbonaceous aerosols in China. The primary biomass-burning emissions
51 accounted for 40±8%, 48±18%, 53±4% and 65±26% of non-fossil OC for Xian, Beijing,
52 Shanghai and Guangzhou, respectively. Other non-fossil sources excluding primary biomass-
53 burning were mainly attributed to formation of secondary organic carbon (SOC) from non-fossil
54 precursors such as biomass-burning emissions. For each site, we also compared samples from
55 moderately with heavily polluted days according to particulate matter mass. Despite a significant
56 increase of absolute mass concentrations of primary emissions from both ~~-,~~ fossil and non-fossil
57 sources, during the heavily polluted events, their relative contribution to TC was even decreased,
58 whereas the portion of SOC was consistently increased at all sites. This observation indicates that
59 SOC was an important fraction in the increment of carbonaceous aerosols during the haze episode
60 in China.

61 1 Introduction

62 Driven by continuous urbanization and industrialization and a rapid growth in the number of
63 motor vehicles and energy consumption, large-scale severe air pollution episodes often affect
64 most cities in China. An increase in the number of haze days is expected to have an adverse
65 impact on human health (Chan and Yao, 2008). Atmospheric fine particles such as PM_{2.5}
66 (particulate matter with an aerodynamic diameter of below 2.5 μm) have been reported as an
67 important air pollutant in China (Donkelaar et al., 2010; Yang et al., 2011; Cao et al., 2012;
68 Huang et al., 2013; Zhao et al., 2013), and its burden is much higher than the 24h-mean of 25
69 μg/m³ suggested by the Air Quality Guidelines of the of World Health Organization (WHO)
70 (WHO, 2006).

71 Carbonaceous aerosols are a major fraction of PM_{2.5} contributing 20-50% of the total PM
72 mass in China's urban atmosphere (Cao et al., 2007). In addition to health and visibility effects,
73 carbonaceous aerosols also influence the earth's climate directly by scattering and absorbing solar
74 radiation and indirectly by modifying cloud microphysics (Pöschl, 2005; IPCC, 2013).
75 Carbonaceous aerosols can be classified into elemental carbon (EC) and organic carbon (OC). EC
76 is exclusively emitted as primary aerosols from incomplete combustion of fossil fuels and
77 biomass burning, whereas OC is a complex mixture of primary directly emitted OC particles
78 (POC) and secondary OC (SOC) formed in-situ in the atmosphere via the oxidation of gas-phase
79 precursors (Pöschl, 2005). POC and precursors of SOC may stem from a vast variety of sources
80 from both anthropogenic (e.g. coal combustion, vehicle emissions and cooking) and natural
81 sources (e.g. biogenic emissions) (Carlton et al., 2009). These sources change over time and
82 space, which makes source apportionment difficult.

83 Several techniques have been applied to quantify the emission sources of carbonaceous
84 aerosols. Radiocarbon (¹⁴C) measurements provide a powerful tool for unambiguously
85 determining fossil and non-fossil sources of carbonaceous particles, since ¹⁴C is completely
86 depleted in fossil-fuel emissions due to its age (half-life 5730 years), whereas non-fossil carbon
87 sources (e.g. biomass burning, cooking or biogenic emissions) show a contemporary ¹⁴C content
88 (Szidat, 2009; Heal, 2014). Moreover, a better ¹⁴C-based source apportionment can be obtained,
89 when ¹⁴C determinations are performed on OC and EC separately, since EC originates exclusively
90 from combustion of biomass and fossil fuels (Szidat et al., 2006; Szidat, 2009; Bernardoni et al.,
91 2013; Liu et al., 2013; Zhang et al., 2013). However, as both biogenic and biomass-burning OC
92 contain ¹⁴C on the contemporary level, it is still difficult to quantify the contribution from these
93 two sources to OC by ¹⁴C measurements alone. When these are combined with OC/EC and

94 organic marker measurements, the primary and secondary origins of the fossil and non-fossil
95 fractions can be identified (Szidat et al., 2006; Szidat et al., 2007; Szidat et al., 2009; Minguillón
96 et al., 2011; Yttri et al., 2011). In particular, levoglucosan, a thermal degradation product of
97 cellulose combustion, can be used as molecular marker to identify primary biomass-burning
98 emissions (Simoneit et al., 1999; Puxbaum et al., 2007; Viana et al., 2013).

99 During January 2013, the severe problem of air pollution in China became a worldwide
100 concern, as extremely high concentrations of 24-h PM2.5 (i.e. often >100 μm^3) were reported
101 in several large cities affecting ~ 1.3 million km^2 and ~ 800 million people. To investigate sources
102 and formation mechanisms of fine carbonaceous aerosols from this high pollution episode across
103 China, an intensive field experiment was carried out in the four large cities Xian, Beijing,
104 Shanghai and Guangzhou, each of them located in different climatic regions, i.e. central-
105 northwest region, Beijing-Tianjin region, Yangtze Delta Region, and Pearl River Delta Region,
106 respectively. These measurements were used in conjunction with ~~an effective statistical approach~~,
107 Latin-hypercube sampling (LHS) (Gelencsér et al., 2007), to elucidate the origins of the
108 carbonaceous aerosol during the haze event.

109 **2 Methods**

110 **2.1 Sampling**

111 Measurement sites are located in Xian, Beijing, Shanghai and Guangzhou, the representative
112 cities of the central-northwest region, Beijing-Tianjin region, Yangtze Delta Region, and Pearl
113 River Delta Region, respectively. In these regions, haze events frequently occur during winter,
114 when weather conditions trap pollutants over the plain. Detailed descriptions of the sampling sites
115 are given in Table 1. In each city, 24-hour integrated PM2.5 samples were collected on pre-baked
116 quartz filters using high-volume samplers at a flow rate of ~ 1.05 m^3/min from 5 to 25 January
117 2013. The sampling sites are located within campuses of universities or at research centers, >100
118 m away from local sources, such as major roadways, industry or domestic sources. At each
119 sampling site, one field blank sample was collected and analyzed. The results reported here are
120 corrected for corresponding field blanks (Cao et al., 2013). All samples collected were stored at -
121 20 $^\circ\text{C}$ before analysis. The PM2.5 mass on each filter was gravimetrically measured using a
122 temperature and relative humidity controlled microbalance.

123 2.2 Thermal-optical carbon analysis

124 A 1.0 cm² punch from the filter samples is taken for the analysis of the OC and EC mass
125 concentrations by the EUSAAR_2 thermal-optical transmission protocol (Cavalli et al., 2010).
126 The replicate analysis of samples (n = 6) showed a good analytical precision with relative
127 standard deviations of 4.8%, 9.1%, and 5.0% for OC, EC and TC, respectively. The average field
128 blank of OC was 2.0 ± 1.0 µg/cm² (equivalent to ~0.5 µg/m³), which was subtracted from the
129 measured OC concentrations. A corresponding EC blank was not detectable.

130 2.3 ¹⁴C analysis of the carbonaceous fractions

131 Six filters ~~are~~were selected per sampling site for ¹⁴C analysis, three from days with a very
132 high PM loading and three representing an average loading, which are described in Table S1 in
133 the supplement. A thermo-optical OC/EC analyzer (Model4L, Sunset Laboratory Inc, USA)
134 equipped with a non-dispersive infrared (NDIR) detector is used for the isolation of different
135 carbon fractions for subsequent ¹⁴C measurements using a four-step thermo-optical protocol
136 Swiss_4S. The method is described in detail elsewhere (Zhang et al., 2012). For EC isolation,
137 filter samples are first treated by water extraction to remove water-soluble OC to minimize the
138 positive artefact from OC charring to the ¹⁴C result of EC. To remove both non-refractory and
139 refractory OC fractions, the water-extracted filters are then combusted or heated in the following
140 3 steps: step 1 in an oxidizing atmosphere (O₂, 99.9995%) at 375 °C for 150s; step 2 in O₂ at
141 475 °C for 180s; step 3 in helium, at 450 °C for 180s followed by at 650 °C for 180s. Finally, EC
142 is isolated by the combustion of the remaining carbonaceous material at 760 °C within 150s in
143 O₂. This method is optimized to minimize a possible negative EC artifact due to losses of the least
144 refractory EC in the OC removal steps prior to EC collection. In a recent study, we found that the
145 aforementioned negative artefact due to premature EC loss during a harsh OC removal procedure
146 (e.g. combustion of samples at 375 °C for 4 h or longer) before EC isolation potentially
147 underestimates biomass-burning EC contribution by up to ~70%, if only small amounts of EC are
148 recovered (Zhang et al., 2012). The EC recovery for ¹⁴C measurement in this work is 78±10%. A
149 bias from underestimation of biomass burning EC caused by the EC loss of 22 ±10% is corrected
150 using the approach described by Zhang et al. (2012). For TC samples, the filters are combusted
151 using the whole Swiss_4S protocol without OC/EC separation. After the combustion/separation
152 of the desired carbonaceous aerosol fractions (i.e. TC or EC), the resulting CO₂ is trapped
153 cryogenically and sealed in glass ampoules for ¹⁴C measurement, which is conducted by a
154 tabletop accelerator mass spectrometry (AMS) system MICADAS using a gas ion source (Wacker

155 et al., 2013) at the Laboratory for the Analysis of Radiocarbon with AMS (LARA), University of
156 Bern, Switzerland (Szidat et al., 2014). ^{14}C results are expressed as fractions of modern (f_M), i.e.
157 the fraction of the $^{14}\text{C}/^{12}\text{C}$ ratio of the sample related to the isotopic ratio of the reference year
158 1950 (Stuiver and Polach, 1977). This data is then corrected for ^{14}C decay during the period
159 between 1950 and 2013, i.e. the year of measurement. The uncertainties of $f_M(\text{EC})$ and $f_M(\text{TC})$ are
160 <5% and <2%, respectively. ^{14}C results in OC ($f_M(\text{OC})$) is not measured directly, but calculated
161 by:

$$162 \quad f_M(\text{OC}) = \frac{\text{TC} \times f_M(\text{TC}) - \text{EC} \times f_M(\text{EC})}{\text{OC}} \quad (1)$$

163 The uncertainty of $f_M(\text{OC})$ estimated by this approach is on average 8% obtained from an
164 error propagation and include all the individual uncertainties of the $f_M(\text{TC})$ (2%), $f_M(\text{EC})$ (5%),
165 TC (8%) and EC (25%). The uncertainty of $f_M(\text{OC})$ estimated by this approach is <5%. No blank
166 corrections are made for determination of ^{14}C , as the different carbonaceous fractions
167 contributions from field blanks are all less than 2% and thus can be neglected.

168 **2.4 Anhydrosugars and water-soluble potassium measurements**

169 The anhydrosugars (levoglucosan and mannosan) are measured by a recently developed in-
170 situ derivatization/thermal desorption gas-chromatography-mass spectrometry method (IDTD-
171 GC-MS) (Schnelle-Kreis et al., 2005; Orasche et al., 2011). Briefly, the filter punches are placed
172 into glass liners suitable for an automated thermal desorption unit. Isotope-labelled standard
173 compounds are spiked onto the filter surface to account for matrix-influences for quantification.
174 Derivatization is performed on the filter by adding of liquid reagent N-methyl-N-(trimethylsilyl)
175 trifluoroacetamide (MSTFA, Macherey-Nagel, Germany). During 16 min of desorption time, in
176 addition an in-situ derivatization with gaseous MSTFA is carried out to quantitatively silylate
177 polar organic compounds and optimize the automated desorption process. Derivatized and
178 desorbed molecules are first trapped on a pre-column before separation by gas chromatography
179 (BPX-5 capillary column, SGE, Australia). The detection and quantification of compounds is
180 carried out on a Pegasus III time-of-flight mass spectrometer (TOF-MS) using the ChromaTOF
181 software package (LECO, St. Joseph, MI).

182 Concentrations of water-soluble potassium (K^+) and other ions are analyzed with ion
183 chromatography (850 Professional IC, Metrohm, Switzerland) after leaching of a 1.0 cm^2 punch
184 of the filter samples with 50 g of ultrapure water (18.2 $\text{M}\Omega$ quality) for 30 min at 40°C in an
185 ultrasonic bath.

186 2.5 Source apportionment methodology

187 Source apportionment results are obtained by ~~an effective statistical approach known as~~
188 Latin-hypercube sampling (LHS) using the dataset from the measured OC, EC, and levoglucosan
189 mass concentrations, estimated emission ratios as well as ¹⁴C contents of OC and EC. The LHS
190 methodology which is comparable to Monte Carlo simulation was first proposed by (Gelencsér et
191 al., 2007) and later applied in many European sites (e.g. Szidat et al. (2009), Yttri et al. (2011),
192 Gilardoni et al. (2011) and Genberg et al. (2011)). Briefly, central values with low and high limits
193 are associated to all uncertain input parameters (Table 2). Due to the lack of information on the
194 input factors, parameters are assigned equally between the low limit and the central value and
195 between the central value and the high limit. All combinations of parameters are included in
196 frequency distributions of possible solutions except those producing negative values. The
197 approach used here is slightly modified compared to previous studies and briefly summarized in
198 the following.

199 EC arises from biomass burning (EC_{bb}) and fossil-fuel combustion (EC_f):

$$200 \quad \text{EC} = \text{EC}_f + \text{EC}_{bb} \quad (2)$$

201 ~~EC_{bb} is calculated from the EC mass concentration, f_M(EC) and a reference value of biomass-~~
202 ~~burning EC (i.e. fraction of modern in EC emitted from biomass-burning sources, f_M(bb))~~ ~~EC_{bb} is~~
203 ~~calculated from the EC mass concentration, f_M(EC) and a ¹⁴C reference value of biomass burning~~
204 ~~(f_M(bb)):~~

$$205 \quad \text{EC}_{bb} = \text{EC} \times \frac{f_M(\text{EC})}{f_M(\text{bb})} \quad (3)$$

206 Analogously, OC is divided into two sub-fractions, OC from fossil fuel (OC_f) and non-fossil
207 emissions (OC_{nf}). ~~To account for the thermonuclear weapon tests of the late 1950s and early~~
208 ~~1960s, OC_{nf} is calculated from the OC mass concentration, f_M(OC) and a ¹⁴C reference value of~~
209 ~~non-fossil emissions (i.e. fraction of modern in OC emitted from non-fossil sources, f_M(nf)).~~
210 ~~whereof the latter is calculated from the OC mass concentration, f_M(OC) and a ¹⁴C reference~~
211 ~~value of non-fossil emissions (f_M(nf)):~~

$$212 \quad \text{OC} = \text{OC}_f + \text{OC}_{nf} \quad (4)$$

$$213 \quad \text{OC}_{nf} = \text{OC} \times \frac{f_M(\text{OC})}{f_M(\text{nf})} \quad (5)$$

214 In addition to this straightforward OC distinction, OC_f and OC_{nf} are semi-quantitatively
215 classified into additional sub-fractions. On the one hand, OC_f is split into primary and secondary
216 OC from fossil sources, i.e. OC_{pri,f} and OC_{sec,f} respectively:

$$217 \quad \text{OC}_f = \text{OC}_{\text{pri},f} + \text{OC}_{\text{sec},f} \quad (6)$$

218 $OC_{pri,f}$ is determined from EC_f and a primary OC/EC emission ratio for fossil-fuel
 219 combustion, i.e. $(OC/EC)_{pri,f}$:

$$220 \quad OC_{pri,f} = EC_f \times \left(\frac{OC}{EC}\right)_{pri,f} \quad (7)$$

221 As fossil-fuel combustion in China is almost exclusively from coal combustion and vehicle
 222 emissions, $(OC/EC)_{pri,f}$ can be determined as:

$$\left(\frac{OC}{EC}\right)_{pri,f} = p \times \left(\frac{OC}{EC}\right)_{pri,cc} + (1-p) \times \left(\frac{OC}{EC}\right)_{pri,ve} \quad (8)$$

223 where p is a percentage of coal combustion in total fossil emissions, and $(OC/EC)_{pri,cc}$ and
 224 $(OC/EC)_{pri,ve}$ a primary OC/EC ratio for coal combustion (cc) and vehicle emissions (ve),
 225 respectively.

226 This strategy can only be applied to OC_{nf} after some modification, as its primary OC/EC
 227 emission ratio is far too uncertain for a general split of non-fossil OC into of primary vs.
 228 secondary formation. Alternatively, OC_{nf} is subdivided into primary biomass burning (OC_{bb}) and
 229 all the other non-fossil sources ($OC_{other,nf}$):

$$230 \quad OC_{nf} = OC_{bb} + OC_{other,nf} \quad (9)$$

231 $OC_{other,nf}$ includes all the other non-fossil sources except OC_{bb} , thus mainly representing
 232 primary and secondary biogenic OC, urban non-fossil contributions (e.g. from cooking or frying)
 233 as well as SOC from biomass burning; due to cholesterol concentrations below the limit of
 234 detection in all samples, however, contributions of cooking and/or frying to $OC_{other,nf}$ can be
 235 neglected. OC_{bb} is calculated by two alternative “marker-to-OC” methods using either EC_{bb} or
 236 levoglucosan (lev) as biomass-burning marker with corresponding primary marker-to-OC
 237 emission ratios (Eq. 9 and 10).

$$238 \quad OC_{bb} = \frac{EC_{bb}}{\left(\frac{EC}{OC}\right)_{bb}} \quad (10)$$

$$OC_{bb} = \frac{lev}{\left(\frac{lev}{OC}\right)_{bb}} \quad (11)$$

239 The overlapping results of both calculations are considered as probable solutions for OC_{bb} .
 240 The consistency of EC_{bb} and levoglucosan data is shown below in Figure 4.

241 Extensive discussion of the selection of the used input parameters can be found in earlier
 242 studies conducted in Europe (e.g. (Gelencsér et al., 2007), (Szidat et al., 2009), (Yttri et al., 2011),
 243 (Gilardoni et al., 2011), (Genberg et al., 2011)). However, due to different conditions in this study,
 244 the input values have to be adapted (Table 2):

- 245 | I. To correct for the ^{14}C bomb peak, the reference values of f_M for biomass burning and non-
246 fossil sources, i.e. $f_M(\text{bb})$ and $f_M(\text{nf})$, respectively, are adapted to the sampling year 2013.
247 $f_M(\text{bb})$ is estimated as 1.10 ± 0.05 using a tree growth model as described in (Mohn et al.,
248 2008). The low limit of $f_M(\text{nf})$ is 1.03, which is equal to the f_M of CO_2 in the atmosphere
249 (Levin et al., 2010), and the high limit of $f_M(\text{nf})$ is set to $f_M(\text{bb})$ with the central value as
250 the average of both.
- 251 II. Literature data indicate that emission ratios depend on fuel types and combustion
252 conditions as well as specific measurement techniques, e.g. for EC mass (Fine et al.,
253 2004; Puxbaum et al., 2007). A range of 0.07-0.20 and 0.10-0.30 is used as the low-to-
254 high values for the $(\text{lev}/\text{OC})_{\text{bb}}$ and $(\text{EC}/\text{OC})_{\text{bb}}$, respectively, covering most of the variation
255 in the measurements and the range used in previous studies (e.g. Gelencser et al. (2007);
256 Genberg et al. (2011); Szidat et al. (2009); Yttri et al. (2011); ~~Genberg et al. (2011)~~).
257 Zhang et al. (2007b) reported an average $(\text{lev}/\text{OC})_{\text{bb}}$ ratio of 0.082 for the main types of
258 Chinese cereal straw (rice, wheat, and corn) based on combustion chamber experiments.
259 As cereal straw is one of the most abundant biomass burned in China, the above ratio
260 (0.082) was used to estimate biomass-burning contribution to OC in Beijing (Zhang et al.,
261 2008) and Hong Kong (Sang et al., 2011). However, this ratio is lower than that (0.14)
262 obtained from the combustion of hardwood in fireplaces and stoves in the US (Fine et al.,
263 2004), which was applied to estimate the contribution of biomass burning to OC at
264 background sites in Europe (Gelencsér et al., 2007; Puxbaum et al., 2007; Schmidl et al.,
265 2008). Considering both main biomass types (i.e. mainly cereal-straw, but also hard-
266 wood burning) (see Sec. 3.2.3), the central value for $(\text{lev}/\text{OC})_{\text{bb}}$ of 0.11 is used in this
267 study. Based on emission factors for primary particulate emissions in China (Zhang et al.,
268 2007), the central value for $(\text{EC}/\text{OC})_{\text{bb}}$ is chosen as 0.22.
- 269 III. $(\text{EC}/\text{OC})_{\text{pri,ve}}$ is determined for emissions from traffic as 0.8-2.1 with the central value of
270 1.45, which is taken from composite profiles from tunnel experiments in Europe
271 (Gelencsér et al., 2007) and the range of this ratio also covers many tunnel studies
272 conducted in China (Huang et al., 2006; He et al., 2008). For $(\text{EC}/\text{OC})_{\text{pri,cc}}$, it ranges for
273 emissions for coal burning in China from 0.32 to 0.62 depending on the share of briquette
274 and chunk bituminous coal with central value of 0.44 for the average coal inventory (Zhi
275 et al., 2008).
- 276 IV. In many urban sites such as Barcelona (Minguillón et al., 2011), Zurich (Szidat et al.,
277 2006) and Pasadena (Zotter et al., 2014), EC_f was almost exclusively attributed to vehicle
278 emissions. However, in China coal combustion is also considered to be an important

Formatted: English (U.S.)

279 contributor to EC emission in winter from both field studies (Cao et al., 2011b) and
280 inventory estimations (Cao et al., 2011a). Recently, Huang et al. (2014) reported relative
281 contribution from coal combustion to total fossil emissions (i.e. p in the Eq (8)) ranges
282 from 0.16-0.80 in Chinese aerosols. In this study, p is assigned as 0-0.7 with the central
283 value of 0.35. It should be noted that for the regions with negligible coal combustion, p
284 can be directly assigned as 0 to simplify this approach. In such a case, $(EC/OC)_{pri,f}$ is
285 equal to $(EC/OC)_{pri,ve}$.

286 To evaluate uncertainties of the quantification of source contributions, the LHS method is
287 implemented to generate 3000 random sets of variables (Gelencsér et al., 2007). A few
288 simulations producing negative solutions are excluded and the median value from the remaining
289 simulations is considered as the best estimate (see Sec 3.2), and the 10th and 90th percentiles of the
290 solutions are treated as uncertainties. These uncertainties typically amount to 13% and 10% for
291 the separation of EC into EC_f and EC_{bb} as well as for OC into OC_f and OC_{nf}, respectively. The
292 uncertainties are higher for the further source apportionment of OC (on the average 25%, 20%,
293 20% and 25% for OC_{pri,f}, OC_{sec,f}, OC_{bb} and OC_{other,nf}, respectively). The ¹⁴C analysis performed on
294 the EC fraction directly enables a more reliable quantification of fossil and biomass burning EC
295 compared to those results obtained by many previous studies (e.g. Gelencser et al., 2007; Yttri et
296 al., 2011; Genberg et al., 2011), in which ¹⁴C analysis were only conducted on TC samples alone.
297 The results of the sensitivity analysis and the determination of the uncertainties will be discussed
298 further in Sec. 3.2.4. The comparison of the ¹⁴C approach with other organic makers (see Sec
299 3.2.3) as well as with the source apportionment results from positive matrix factorization (Paatero
300 and Tapper, 1994) using the multi-linear engine (ME-2) algorithm (Paatero and Hopke, 2009)
301 (see Sec. 3.3.3) will provide additional measures to evaluate the model performance.

302 **3 Results and discussions**

303 **3.1 PM2.5 and carbonaceous aerosols mass concentrations**

304 The whisker box plots (Figure 1) show the concentrations of PM2.5, OC and EC as well as
305 EC to OC ratios (EC/OC) in the four Chinese cities. The average PM2.5 mass concentrations at
306 the Xian, Beijing, Shanghai, and Guangzhou sampling sites during the sampling periods were
307 345±125 µg/m³, 158±81 µg/m³, 90±31 µg/m³, and 68±23 µg/m³, respectively. Despite large
308 variations in the PM2.5 concentrations within each site, their concentrations were always higher
309 in Xian and Beijing compared to those in Shanghai and Guangzhou, reflecting a poorer air quality

310 in Northern China. Extremely high PM_{2.5} concentrations were observed for several days during
311 the sampling period. The highest 24-h average PM_{2.5} value (134-517 $\mu\text{g}/\text{m}^3$) was 5-20 times
312 higher than the WHO guideline for 24-h PM_{2.5} (25 $\mu\text{g}/\text{m}^3$, (WHO, 2006)). Only 3% of PM_{2.5}
313 mass values were below this guideline value, indicating a very high negative impact on human
314 health in all studied cities.

315 OC and EC concentrations showed similar spatial distributions as the PM_{2.5} mass in the
316 order: Xian>Beijing>Shanghai>Guangzhou. Given that average temperatures during the sampling
317 period were 10-20°C lower in Xian and Beijing than in Shanghai and Guangzhou, the high
318 concentrations of carbonaceous species in northern cities could be due to enhanced fuel
319 consumption for heating activities (Weilenmann et al., 2009; Nordin et al., 2013). The EC/OC
320 ratios were comparable for Xian, Shanghai and Guangzhou, but considerably lower at Beijing.

321 We also compared the data of OC, EC and EC/OC from heavily polluted days with
322 moderately polluted days, which were selected from the samples with the highest and average PM
323 loading, respectively (Table 3). ¹⁴C measurements were also performed on these samples (Sect.
324 2.3), and a detailed source apportionment result will be presented in Sect. 3.2. The PM_{2.5}, OC
325 and EC mass concentrations on heavily polluted days were mostly >2 times as high as those on
326 moderately polluted days at the four sites. On the heavily polluted days, the EC/OC ratios
327 significantly decreased by 29% and 43% in northern cities of Xian and Beijing, respectively,
328 whereas they slightly increased in Shanghai and Guangzhou by 13% and 16%, respectively. The
329 higher PM_{2.5} mass, OC and EC observed during the polluted period was characterized by low
330 wind speed but not significantly sensitive by the temperature and relative humidity.

331 **3.2 Best estimate of source apportionment results**

332 **3.2.1 Fossil and biomass burning EC**

333 Figure 2 shows the source apportionment results of EC. The concentration of EC from fossil-
334 fuel sources (EC_f) ranged from 0.61 to 16.8 $\mu\text{g}/\text{m}^3$, whereas the corresponding range for EC from
335 biomass burning (EC_{bb}) was 0.57 to 4.71 $\mu\text{g}/\text{m}^3$. EC_f values were on average 3 times as high as
336 EC_{bb} , corresponding to a mean fraction of EC_f to total EC of 0.75. The highest concentrations of
337 EC_{bb} and EC_f were observed in Xian, followed by Beijing and the two southern sites Shanghai
338 and Guangzhou.

339 Despite the wide range of EC concentrations, the fraction of EC_f to total EC in Xian, Beijing
340 and Shanghai was fairly constant with average values of $78\pm 3\%$, $76\pm 4\%$ and $79\pm 4\%$,
341 respectively. This finding suggests that the increase of EC_f and EC_{bb} emissions in the three cities

342 on the heavily polluted days is likely due to ~~an equal enhancement of fossil fuel and biomass-~~
343 ~~burning combustion emissions and~~ the accumulation of ~~these particulate~~ pollutants, ~~during winter~~
344 ~~with an equally enhancement of fossil fuel and biomass burning combustion emissions.~~ At
345 Guangzhou, however, the EC_f contribution was noticeably higher on the heavily (i.e. $80\pm 2\%$)
346 compared to the moderately polluted days (i.e. $57\pm 5\%$), indicating that the increase of the EC
347 concentrations was rather caused by additional fossil-fuel emissions than by biomass burning.
348 The measured fossil contributions to EC correspond to those previously reported at 3 city sites
349 and 2 regional sites in China (Chen et al., 2013), but are higher than for the Maldives ($31\pm 5\%$),
350 India ($36\pm 3\%$) (Gustafsson et al., 2009) and a background site on the South Chinese island
351 Hainan ($25\text{-}56\%$) (Zhang et al., 2014a).

352 3.2.2 Fossil and non-fossil OC

353 The concentration of OC from fossil-fuel sources (OC_f) ranged from 2.53 to $61.3 \mu\text{g}/\text{m}^3$,
354 whereas the corresponding range for OC from non-fossil sources (OC_{nf}) was 0.8 to $42.7 \mu\text{g}/\text{m}^3$
355 (Figure 3). Similar to EC, the highest mean concentrations of OC_f and OC_{nf} were both observed at
356 Xian and Beijing. The mean concentration of OC_{nf} was higher than that of OC_f for all sites except
357 Beijing. OC_f contributions (mean \pm standard deviation) to total OC were $37\pm 3\%$, $58\pm 5\%$, $49\pm 2\%$
358 and $35\pm 8\%$ in Xian, Beijing, Shanghai and Guangzhou, respectively, which was lower than the
359 corresponding EC_f fraction to EC for all samples (Figure 2). The high percentage of OC_{nf}
360 demonstrates that even in densely populated and urbanized areas of China, non-fossil sources are
361 still a considerable and sometimes even a dominant contributor of OC, at least in winter. The
362 large variability of the fraction of OC_f to total OC ~~for-among~~ the different cities furthermore
363 reflects complex sources and formation processes of OC_f . In addition, the ratio of EC_f ~~and-to~~ OC_f
364 $(EC/OC)_f$ in Beijing (0.24 ± 0.10) was substantially lower than in Xian (0.53 ± 0.15), Shanghai
365 (0.47 ± 0.11) and Guangzhou (0.56 ± 0.11), which will be discussed below.

366 3.2.3 Other biomass-burning markers

367 Figure 4 shows that levoglucosan (lev) and mannosan (man) concentrations significantly
368 correlated with EC_{bb} . Their correlation coefficients were 0.87 and 0.92, respectively. In spite of
369 different concentration levels, no significant differences were observed in the slopes among
370 different cities for the different anhydrosugars or pollution levels. A possible explanation is that
371 the burning conditions and fuel type was rather consistent during the sampling period for the four
372 cities. Moreover, the regression slope (0.41 ± 0.03) of levoglucosan and EC_{bb} obtained here was
373 similar to that (0.45) calculated by the ratio of the best estimates of lev/OC (0.10) and EC/OC
374 (0.22) using the LHS simulation (median values in Table 2), indicating that our assumption of

375 LHS input parameters is reasonable. The average lev-to-man ratio was 27.7 ± 8.47 (ranging from
376 16.4 to 45.9), which is at the higher end of the reported ratios for crop residue burning (ranging
377 from 12.9 to 55.7 with a mean of 32.6 ± 19.1) and obviously higher than that from softwood $4.0 \pm$
378 1.0 (ranging from 2.5 to 5.8 with a mean of 4.0 ± 1.0) (Sang et al., 2013). However, the ratio is
379 not significantly different from ratios reported for hardwood burning (ranging from 12.9 to 35.4
380 with a mean of 21.5 ± 8.3) (Sang et al., 2013).

381 Recently, Cheng et al. (2013) proposed that ratios of levoglucosan to another biomass
382 burning marker, non-sea-salt-potassium ($\text{nss-K}^+ = \text{K}^+ - 0.0355 \times \text{Na}^+$, (Lai et al., 2007)), can be
383 used to distinguish biomass burning from crop residue and wood. The average of lev-to- K_{nss}^+ in
384 our study was 0.59 ± 0.33 (ranging from 0.17 to 1.56 with only 2 samples >1), which is
385 comparable to the ratios for wheat straw (0.10 ± 0.00), corn straw (0.21 ± 0.08) and rice straw
386 grown in Asia (0.62 ± 0.32) (Cheng et al., 2013). These ratios are much lower than those ratios
387 reported for hardwood (23.96 ± 1.82) (Cheng et al., 2013). With a combination of the lev-to-man
388 and lev-to- K^+ ratios, it can be concluded that the major source of biomass burning in winter of
389 China is combustion of crop residues. In addition, non-sea-salt-potassium concentrations also
390 show a very good correlation ($R^2=0.82$) with EC_{bb} for the four cities. This also confirms that the
391 variability of burning conditions and biomass types was rather small during winter 2013 in
392 different regions of China.

393 3.2.4 Sensitivity analysis

394 Figure 5 shows the results of the sensitivity test for the average contribution of each source
395 to TC for all sites. Each source is illustrated as a frequency distribution, from which the
396 uncertainties of the source apportionment are deduced as given in Section 2.5. We found that
397 EC_{bb} was always the smallest contributor ($<10\%$), but was still non-negligible for all sites. The
398 distributions of EC_{f} and EC_{bb} were much narrower than for the different OC sources due to the
399 direct ^{14}C determination of EC and the indirect calculation of the OC fractions. OC_{bb} and $\text{OC}_{\text{other,nf}}$
400 were the most uncertain contributors to TC due to the large variation of the input parameters for
401 LHS calculations, i.e. $(\text{EC}/\text{OC})_{\text{bb}}$ and $(\text{lev}/\text{OC})_{\text{bb}}$. Despite a large spread of $\text{OC}_{\text{sec,f}}$ and $\text{OC}_{\text{other,nf}}$,
402 the data conclusively shows that both contributions were always larger on the heavily than on the
403 moderately polluted days, highlighting the importance of fossil-derived SOC formation and other
404 non-fossil emissions excluding primary biomass burning sources. The increased $\text{OC}_{\text{other,nf}}$ is likely
405 due to enhanced SOC formation from biomass burning and other non-fossil sources (see Sec.
406 3.3). ~~Despite a large spread of $\text{OC}_{\text{sec,f}}$ and $\text{OC}_{\text{other,nf}}$, the data conclusively shows that both
407 contributions were always larger on the heavily than on the moderately polluted days,
408 highlighting the importance of SOC formation from both fossil and non-fossil emissions.~~

409 3.3 The relevance of SOC for heavily polluted days

410 3.3.1 Further source apportionment of OC sources

411 As explained in Sec. 2.4, OC_f is apportioned into primary and secondary OC from fossil
412 sources, whereas OC_{nf} is subdivided into primary biomass-burning OC (OC_{bb}) and the other non-
413 fossil OC ($OC_{other,nf}$). As shown in Figure 6, $OC_{sec,f}$ was generally more abundant than $OC_{pri,f}$,
414 suggesting that SOC is the predominant fraction of OC_f in Chinese cities during winter. The
415 highest $OC_{sec,f}$ -to- $OC_{pri,f}$ ratio (with average of 4.2) was found in Beijing, indicating the largest
416 SOC formation compared to the other three sites (average $OC_{sec,f}$ -to- $OC_{pri,f}$ ratio of 1.3), which is
417 in agreement with the higher OC_f/EC_f ratios (see Sect. 3.2.2). During heavily polluted days,
418 $OC_{sec,f}$ -to- $OC_{pri,f}$ ratios increased compared to moderately polluted days on average by 70% for
419 the 4 sites. This underlines that the episodes with bad air quality were mainly caused by
420 additional SOC formation and accumulation of similar pollutants as for average winter
421 conditions. The importance of fossil-derived SOC formation was also underlined by ^{14}C
422 measurement in water-soluble OC during 2011 winter in Beijing and Guangzhou (Zhang et al.,
423 2014b). Figure 6 shows that OC_{bb} was higher than $OC_{other,nf}$ on the moderately polluted days for
424 all sites, while it changed to the contrary on the heavily polluted days. The excess of non-fossil
425 OC concentration for the heavily polluted days was dominated by $OC_{other,nf}$, which was ~2.6 times
426 as high as OC_{bb} . The dominating contribution of $OC_{other,nf}$ is likely due to the increase of SOC
427 formation from non-fossil sources mainly from biomass-burning emissions, although biogenic-
428 derived SOC could not be excluded for SH and GZ where temperatures during the sampling
429 period are above 0 degrees. ~~The dominating contribution of $OC_{other,nf}$ is likely due to the increase
430 of SOC formation from non-fossil sources (i.e. mainly from biomass-burning emissions).~~ In
431 conclusion, the source apportionment results of the excess carbonaceous aerosols consistently
432 highlight the importance of SOC from both, fossil and non-fossil sources. It should be also noted
433 that the condensation of semi-volatile organic aerosols generally may contribute to some extent to
434 the measured SOA in winter due to the colder temperature in the northern sites such as Beijing
435 and Xian. However, the increased SOA between the MPD and HPD measured by the current
436 method is mostly if not exclusively due to enhanced SOA formation since the temperatures during
437 the moderately and heavily polluted days were not significantly different ($p \gg 0.05$).

438 3.3.2 Relative contribution from OC and EC source categories to TC

439 The contributions of different OC and EC source categories to TC are shown in Table 4.
440 Fossil sources ($EC_f + OC_{pri,f} + OC_{sec,f}$) account for an important contribution at all sites, which
441 decreased from Beijing (60%) to Shanghai (56%), Xian (45%) and Guangzhou (43%). The larger

442 fossil contribution in Beijing can be explained by substantially higher $OC_{sec,f}$ values, which were
443 often >2 times as high as for the other three sites. However, no remarkable difference was found
444 for the total primary fossil contribution ($EC_f+OC_{pri,f}$) between the heavily and the moderately
445 polluted days. An exception of this tendency was observed for Guangzhou, in which the fossil
446 contribution to TC increased by 36% during the polluted episodes. However, the contribution of
447 $OC_{sec,f}$ to TC was higher on the heavily polluted days than on the moderately polluted days for all
448 sites, which indicates a significant contribution of fossil SOC to TC during winter haze or smog
449 episodes in China.

450 Primary biomass-burning sources ($EC_{bb}+OC_{bb}$) were a large contributor to TC (on average
451 25%, 21%, 26% and 39% in Xian, Beijing, Shanghai and Guangzhou, respectively). However, the
452 relative contribution of biomass burning decreased on average from ~28% to ~17% when
453 comparing moderately with heavily polluted days. Therefore, primary biomass-burning emissions
454 were not a major additional source during heavily polluted days.

455 A considerable fraction of TC originated from $OC_{other,nf}$ with a mean contribution of 21% for
456 all sites. The presence of $OC_{other,nf}$ is unlikely attributed to primary or secondary biogenic particles
457 as biogenic emissions are very low during winter at least in Northern China, although these can
458 be enriched due to favoring condensation of SVOCs into the particle phase at colder
459 temperatures. In combination with the observation of enhanced fossil SOC formation, we assume
460 that this excess is mainly attributed to SOC formation from non-fossil, but non-biogenic
461 precursors (i.e. mainly from biomass-burning emissions). Further, SOC formation from these
462 non-fossil volatile organic compounds may be enhanced, when they are mixed with
463 anthropogenic pollutants such as volatile organic compounds (VOCs) and NO_x (Weber et al.,
464 2007; Hoyle et al., 2011).

465 As the $OC_{sec,f}$ and $OC_{other,nf}$ contributions were always considerably higher on the most
466 polluted days compared the moderately polluted days and the increase of primary sources (such
467 as EC_{bb} , OC_{bb} and $OC_{pri,f}$) was less prominent (see Figure 6), we conclude that the increment of
468 TC on the heavily polluted days was mainly driven by the increase of SOC from both fossil fuel
469 and non-fossil emissions. This is also underlined in Figure 6 by the composition of the excess for
470 the heavily polluted days.

471 3.3.3 Comparison with multi-linear engine (ME-2) source apportionment

472 In a parallel study from the same sites and episodes (Huang et al., 2014), the multi-linear
473 engine (ME-2) receptor model (Canonaco et al., 2013) was used to estimate the OC contribution
474 from different factors including coal, traffic, dust-related, cooking and secondary sources. This

475 model includes EC/OC, ions and organic marker compounds (polycyclic aromatic hydrocarbons
476 (PAHs), oxygenated PAHs (o-PAHs), resin acids, anhydrous sugars, lignin pyrolysis products and
477 hopanes) in addition to high resolution Aerodyne aerosol mass spectra from offline analysis of
478 nebulized water-extracts from filter samples by a high-resolution time-of-flight aerosol mass
479 spectrometer, HR-ToF-AMS (Daellenbach et al., *in preparation*). For comparison with the results
480 from this work, sources resolved by the ME-2 approach are further classified into the following
481 basic classes: fossil primary OC (POC_f), non-fossil primary OC (POC_{nf}), fossil secondary OC
482 (SOC_f) and non-fossil secondary OC (SOC_{nf}). Figure 7 shows a significant linear correlation
483 between the two approaches ($p < 0.01$, $n = 24$, all samples are included), underscoring the proper
484 choices of the selected source profiles in this study (i.e. inputs for LHS). A very good agreement
485 between the two methods is found for SOC_{nf} , whereas an offset deviation of $\sim 13\%$ occurs for
486 SOC_f possibly due to uncertainties in both models. It is important to note that such a difference is
487 not observed ($p < 0.01$), if we exclude the data from Beijing. And SOC_f may be overestimated, if
488 we underestimate the contribution of coal combustion to fossil-fuel derived EC (p in Eq. (8)) in
489 Beijing. The findings of Huang et al. (2014) suggest that coal combustion is substantially higher
490 in this city compared to the other sites. Increasing the value of p by a factor of 2 (i.e. from 0.35 to
491 0.70) for Beijing decreases the contribution of SOC_f to the benefit of POC_f , whereas the other
492 components (EC_f , EC_{bb} , OC_{bb} , $OC_{other,nf}$) are independent of the choice of the p value (see Tab. S2
493 and Fig. S1). This modification improves the agreement of SOC_f between both approaches as
494 shown in Fig. 7. Furthermore, it decreases the $OC_{sec,f}$ -to- $OC_{pri,f}$ ratio of Beijing from 2.7 and 5.9
495 to 1.2 and 2.9 for the moderately and heavily polluted daysMPD and HPD, respectively. As a
496 consequence, these values become better comparable with those of the other cities, but still
497 underline the importance of secondary aerosol formation during the heavily polluted daysHPD.

498 **4 Conclusions**

499 Source apportionment of the carbonaceous aerosol in PM_{2.5} during a severe winter pollution
500 episode of 2013 in China was conducted at four major cities including Xian, Beijing, Shanghai
501 and Guangzhou. An effective sStatistical analysis of concentrations of OC and EC, anhydrosugars
502 as well as ¹⁴C contents of OC and EC using Latin-hypercube sampling (LHS) allowed a
503 quantitative estimation of six different sources. These sources included EC from combustion of
504 biomass (EC_{bb}) and fossil fuels (EC_f), OC from fossil emissions including primary and secondary
505 sources (i.e. $OC_{pri,f}$ and $OC_{sec,f}$, respectively) as well as OC from non-fossil sources including
506 primary biomass burning and all the other non-fossil OC (i.e. OC_{bb} and $OC_{other,nf}$, respectively). A
507 sensitivity analysis of the LHS simulation showed the robustness of our results, as the uncertainty

508 of the different emission sources was usually below 20% of TC, which was mainly achieved by
509 the combination of different isotopic and molecular markers.

510 Fossil emissions predominated EC with a mean contribution of $75\pm 8\%$ at all sites. The
511 remaining $25\pm 8\%$ was attributed to biomass-burning sources, and the presence of the latter was
512 also confirmed by other biomass-burning markers such as levoglucosan and water-soluble
513 potassium. The fossil contribution to OC was lower than for EC and was highest in Beijing
514 ($58\pm 5\%$) and decreased in the order: Shanghai ($49\pm 2\%$) > Xian ($38\pm 3\%$) > Guangzhou ($35\pm 7\%$).

515 Conversely, non-fossil sources accounted on the average for $55\pm 10\%$ and $48\pm 9\%$ of OC and
516 TC, respectively. Air pollution from the neighboring rural regions may have contributed
517 substantially to non-fossil carbon of urban aerosols, as biofuel usage is more common for heating
518 and cooking in such regions during winter time in China. The average contribution of non-fossil
519 OC from OC_{bb} was found to $40\pm 8\%$, $48\pm 18\%$, $53\pm 4\%$ and $65\pm 26\%$ for Xian, Beijing, Shanghai
520 and Guangzhou, respectively.

521 A considerable fraction of OC was identified as SOC. We found that $OC_{sec,f}$ dominated over
522 $OC_{pri,f}$ for all samples (i.e. portions of TC of $23\pm 11\%$ compared to $13\pm 3\%$, respectively), strongly
523 implying importance of fossil-derived SOC to urban (often polluted) aerosols in China.
524 Furthermore, we classified the samples into 2 episodes, heavily polluted and moderately polluted
525 days, depending on PM mass. We found the relative $OC_{other,nf}$ contributions tend to be higher on
526 the heavily polluted days at all sites, which were mainly attributed to enhanced SOC formation
527 from non-fossil precursors such as biomass-burning emissions. Even though a significant increase
528 of absolute mass concentrations of primary emissions (both fossil and non-fossil sources) was
529 found on the heavily compared to moderately polluted days, their relative contribution to TC was
530 even decreased, while SOC contributions from both fossil and non-fossil sources were
531 substantially increased. This finding was consistently observed for all sites, showing the
532 importance of SOC during severe haze events in China.

533 **Acknowledgement**

534 Yanlin Zhang acknowledges partial support from the Swiss National Science Foundation
535 Fellowship.

536 **References**

537 Bernardoni, V., Calzolari, G., Chiari, M., Fedi, M., Lucarelli, F., Nava, S., Piazzalunga, A.,
538 Riccobono, F., Taccetti, F., Valli, G., and Vecchi, R.: Radiocarbon analysis on organic and

539 elemental carbon in aerosol samples and source apportionment at an urban site in Northern
540 Italy, *J. Aerosol Sci.*, 56, 88-99, 2013.

541 Canonaco, F., Crippa, M., Slowik, J. G., Baltensperger, U., and Prévôt, A. S. H.: SoFi, an IGOR-
542 based interface for the efficient use of the generalized multilinear engine (ME-2) for the
543 source apportionment: ME-2 application to aerosol mass spectrometer data, *Atmos. Meas.*
544 *Tech.*, 6, 3649-3661, 2013.

545 Cao, F., Zhang, Y.-L., Szidat, S., Zapf, A., Wacker, L., and Schwikowski, M.: Microgram level
546 radiocarbon determination of carbonaceous particles in firn samples: pre-treatment and
547 OC/EC separation, *Radiocarbon*, 55, 383-390 2013.

548 Cao, G. L., Zhang, X. Y., Gong, S. L., An, X. Q., and Wang, Y. Q.: Emission inventories of
549 primary particles and pollutant gases for China, *Chin. Sci. Bull.*, 56, 781-788, 2011a.

550 Cao, J.-j., Chow, J. C., Tao, J., Lee, S.-c., Watson, J. G., Ho, K.-f., Wang, G.-h., Zhu, C.-s., and
551 Han, Y.-m.: Stable carbon isotopes in aerosols from Chinese cities: Influence of fossil fuels,
552 *Atmos. Environ.*, 45, 1359-1363, 2011b.

553 Cao, J. J., Lee, S. C., Chow, J. C., Watson, J. G., Ho, K. F., Zhang, R. J., Jin, Z. D., Shen, Z. X.,
554 Chen, G. C., Kang, Y. M., Zou, S. C., Zhang, L. Z., Qi, S. H., Dai, M. H., Cheng, Y., and Hu,
555 K.: Spatial and seasonal distributions of carbonaceous aerosols over China, *J. Geophys. Res.*,
556 112, D22S11, 2007.

557 Cao, J. J., Shen, Z. X., Chow, J. C., Watson, J. G., Lee, S. C., Tie, X. X., Ho, K. F., Wang, G. H.,
558 and Han, Y. M.: Winter and summer PM_{2.5} chemical compositions in fourteen chinese cities,
559 *J. Air Waste Manage. Assoc.*, 62, 1214-1226, 2012.

560 Carlton, A. G., Wiedinmyer, C., and Kroll, J. H.: A review of Secondary Organic Aerosol (SOA)
561 formation from isoprene, *Atmos. Chem. Phys.*, 9, 4987-5005, 2009.

562 Cavalli, F., Viana, M., Yttri, K. E., Genberg, J., and Putaud, J. P.: Toward a standardised thermal-
563 optical protocol for measuring atmospheric organic and elemental carbon: the EUSAAR
564 protocol, *Atmos. Meas. Tech.*, 3, 79-89, 2010.

565 Chan, C. K., and Yao, X.: Air pollution in mega cities in China, *Atmos. Environ.*, 42, 1-42, 2008.

566 Chen, B., Andersson, A., Lee, M., Kirillova, E. N., Xiao, Q., Krusa, M., Shi, M., Hu, K., Lu, Z.,
567 Streets, D. G., Du, K., and Gustafsson, O.: Source forensics of black carbon aerosols from
568 china, *Environ. Sci. Technol.*, 47, 9102-9108, 2013.

569 Cheng, Y., Engling, G., He, K. B., Duan, F. K., Ma, Y. L., Du, Z. Y., Liu, J. M., Zheng, M., and
570 Weber, R. J.: Biomass burning contribution to Beijing aerosol, *Atmos. Chem. Phys.*, 13,
571 7765-7781, 2013.

572 Donkelaar, A. v., Martin, R. V., Brauer, M., Kahn, R., Levy, R., Verduzco, C., and Villeneuve, P.

573 J.: Global estimates of ambient fine particulate matter concentrations from satellite-based
574 aerosol optical depth: development and application, *Environ. Health Perspect.*, 118, 847,
575 2010.

576 Fine, P. M., Cass, G. R., and Simoneit, B. R. T.: Chemical characterization of fine particle
577 emissions from the wood stove combustion of prevalent United States tree species, *Environ.*
578 *Eng. Sci.*, 21, 705-721, 2004.

579 Gelencsér, A., May, B., Simpson, D., Sánchez-Ochoa, A., Kasper-Giebl, A., Puxbaum, H.,
580 Caseiro, A., Pio, C., and Legrand, M.: Source apportionment of PM_{2.5} organic aerosol over
581 Europe: Primary/secondary, natural/anthropogenic, and fossil/biogenic origin, *J. Geophys.*
582 *Res.*, 112, D23S04, 2007.

583 Genberg, J., Hyder, M., Stenström, K., Bergström, R., Simpson, D., Fors, E., Jönsson, J. Å., and
584 Swietlicki, E.: Source apportionment of carbonaceous aerosol in southern Sweden, *Atmos.*
585 *Chem. Phys.*, 11, 11387-11400, 2011.

586 Gilardoni, S., Vignati, E., Cavalli, F., Putaud, J. P., Larsen, B. R., Karl, M., Stenström, K.,
587 Genberg, J., Henne, S., and Dentener, F.: Better constraints on sources of carbonaceous
588 aerosols using a combined ¹⁴C-macro tracer analysis in a European rural background site,
589 *Atmos. Chem. Phys.*, 11, 5685-5700, 2011.

590 Gustafsson, O., Krusa, M., Zencak, Z., Sheesley, R. J., Granat, L., Engstrom, E., Praveen, P. S.,
591 Rao, P. S., Leck, C., and Rodhe, H.: Brown clouds over South Asia: biomass or fossil fuel
592 combustion?, *Science*, 323, 495-498, 2009.

593 He, L. Y., Hu, M., Zhang, Y. H., Huang, X. F., and Yao, T. T.: Fine particle emissions from on-
594 road vehicles in the Zhujiang Tunnel, China, *Environ. Sci. Technol.*, 42, 4461-4466, 2008.

595 Heal, M.: The application of carbon-14 analyses to the source apportionment of atmospheric
596 carbonaceous particulate matter: a review, *Anal. Bioanal. Chem.*, 406, 81-98, 2014.

597 Hoyle, C. R., Boy, M., Donahue, N. M., Fry, J. L., Glasius, M., Guenther, A., Hallar, A. G., Hartz,
598 K. H., Petters, M. D., Petaja, T., Rosenoern, T., and Sullivan, A. P.: A review of the
599 anthropogenic influence on biogenic secondary organic aerosol, *Atmos. Chem. Phys.*, 11,
600 321-343, 2011.

601 Huang, K., Zhuang, G., Lin, Y., Wang, Q., Fu, J. S., Fu, Q., Liu, T., and Deng, C.: How to
602 improve the air quality over megacities in China: pollution characterization and source
603 analysis in Shanghai before, during, and after the 2010 World Expo, *Atmos. Chem. Phys.*, 13,
604 5927-5942, 2013.

605 Huang, R.-J., Zhang, Y., Bozzetti, C., Ho, K.-F., Cao, J., Han, Y., Dällenbach, K. R., Slowik, J.
606 G., Platt, S. M., Canonaco, F., Zotter, P., Wolf, R., Pieber, S. M., Bruns, E. A., Crippa, M.,

607 Ciarelli, G., Piazzalunga, A., Schwikowski, M., Abbaszade, G., Schnelle-Kreis, J.,
608 Zimmermann, R., An, Z., Szidat, S., Baltensperger, U., Haddad, I. E., and Prévôt, A. S. H.:
609 High secondary aerosol contribution to particulate pollution during haze events in China,
610 *Nature*, *In press*, 2014.

611 Huang, X. F., Yu, J. Z., He, L. Y., and Hu, M.: Size distribution characteristics of elemental
612 carbon emitted from Chinese vehicles: Results of a tunnel study and atmospheric
613 implications, *Environ. Sci. Technol.*, *40*, 5355-5360, 2006.

614 IPCC: Climate change 2013: The physical science basis. contribution of working group I to the
615 fifth assessment report of the intergovernmental panel on climate change, Cambridge
616 University Press, Cambridge, United Kingdom and New York, NY, USA, 1533 pp., 2013.

617 Lai, S. c., Zou, S. c., Cao, J. j., Lee, S. c., and Ho, K. f.: Characterizing ionic species in PM_{2.5} and
618 PM₁₀ in four Pearl River Delta cities, South China, *Journal of Environmental Sciences*, *19*,
619 939-947, 2007.

620 Levin, I., Naegler, T., Kromer, B., Diehl, M., Francey, R. J., Gomez-Pelaez, A. J., Steele, L. P.,
621 Wagenbach, D., Weller, R., and Worthy, D. E.: Observations and modelling of the global
622 distribution and long-term trend of atmospheric ¹⁴CO₂, *Tellus Series B*, *62*, 26-46, 2010.

623 Liu, D., Li, J., Zhang, Y., Xu, Y., Liu, X., Ding, P., Shen, C., Chen, Y., Tian, C., and Zhang, G.:
624 The use of levoglucosan and radiocarbon for source apportionment of PM_{2.5} carbonaceous
625 aerosols at a background site in East China, *Environ. Sci. Technol.*, *47*, 10454-10461, 2013.

626 Minguillón, M. C., Perron, N., Querol, X., Szidat, S., Fahrni, S. M., Alastuey, A., Jimenez, J. L.,
627 Mohr, C., Ortega, A. M., Day, D. A., Lanz, V. A., Wacker, L., Reche, C., Cusack, M., Amato,
628 F., Kiss, G., Hoffer, A., Decesari, S., Moretti, F., Hillamo, R., Teinila, K., Seco, R., Penuelas,
629 J., Metzger, A., Schallhart, S., Muller, M., Hansel, A., Burkhardt, J. F., Baltensperger, U., and
630 Prevot, A. S. H.: Fossil versus contemporary sources of fine elemental and organic
631 carbonaceous particulate matter during the DAURE campaign in Northeast Spain, *Atmos.*
632 *Chem. Phys.*, *11*, 12067-12084, 2011.

633 Mohn, J., Szidat, S., Fellner, J., Rechberger, H., Quartier, R., Buchmann, B., and Emmenegger,
634 L.: Determination of biogenic and fossil CO₂ emitted by waste incineration based on ¹⁴CO₂
635 and mass balances, *Bioresour. Technol.*, *99*, 6471-6479, 2008.

636 Nordin, E., Eriksson, A., Roldin, P., Nilsson, P., Carlsson, J., Kajos, M., Hellén, H., Wittbom, C.,
637 Rissler, J., and Löndahl, J.: Secondary organic aerosol formation from idling gasoline
638 passenger vehicle emissions investigated in a smog chamber, *Atmos. Chem. Phys.*, *13*, 6101-
639 6116, 2013.

640 Orasche, J., Schnelle-Kreis, J., Abbaszade, G., and Zimmermann, R.: Technical Note: In-situ

641 derivatization thermal desorption GC-TOFMS for direct analysis of particle-bound non-polar
642 and polar organic species, *Atmos. Chem. Phys.*, 11, 8977-8993, 2011.

643 Paatero, P., and Tapper, U.: Positive matrix factorization - A nonnegative factor model with
644 optimal utilization of error-estimates of data values, *Environmetricsz*, 5, 111-126, 1994.

645 Paatero, P., and Hopke, P. K.: Rotational tools for factor analytic models, *J. Chemom.*, 23, 91-
646 100, 2009.

647 Pöschl, U.: Atmospheric aerosols: composition, transformation, climate and health effects,
648 *Angew. Chem., Int. Ed.*, 44, 7520-7540, 2005.

649 Puxbaum, H., Caseiro, A., Sánchez-Ochoa, A., Kasper-Giebl, A., Claeys, M., Gelencsér, A.,
650 Legrand, M., Preunkert, S., and Pio, C.: Levoglucosan levels at background sites in Europe
651 for assessing the impact of biomass combustion on the European aerosol background, *J.*
652 *Geophys. Res.*, 112, D23S05, 2007.

653 Sang, X. F., Chan, C. Y., Engling, G., Chan, L. Y., Wang, X. M., Zhang, Y. N., Shi, S., Zhang, Z.
654 S., Zhang, T., and Hu, M.: Levoglucosan enhancement in ambient aerosol during springtime
655 transport events of biomass burning smoke to Southeast China, *Tellus Series B-Chemical and*
656 *Physical Meteorology*, 63, 129-139, 2011.

657 Sang, X. F., Zhang, Z. S., Chan, C. Y., and Engling, G.: Source categories and contribution of
658 biomass smoke to organic aerosol over the southeastern Tibetan Plateau, *Atmos. Environ.*, 78,
659 113-123, 2013.

660 Schmidl, C., Marr, I. L., Caseiro, A., Kotianová, P., Berner, A., Bauer, H., Kasper-Giebl, A., and
661 Puxbaum, H.: Chemical characterisation of fine particle emissions from wood stove
662 combustion of common woods growing in mid-European Alpine regions, *Atmos. Environ.*,
663 42, 126-141, 2008.

664 Schnelle-Kreis, J., Sklorz, M., Peters, A., Cyrys, J., and Zimmermann, R.: Analysis of particle-
665 associated semi-volatile aromatic and aliphatic hydrocarbons in urban particulate matter on a
666 daily basis, *Atmos. Environ.*, 39, 7702-7714, 2005.

667 Simoneit, B. R. T., Schauer, J. J., Nolte, C. G., Oros, D. R., Elias, V. O., Fraser, M. P., Rogge, W.
668 F., and Cass, G. R.: Levoglucosan, a tracer for cellulose in biomass burning and atmospheric
669 particles, *Atmos. Environ.*, 33, 173-182, 1999.

670 Stuiver, M., and Polach, H. A.: Discussion: Reporting of ^{14}C data, *Radiocarbon*, 19, 355-363,
671 1977.

672 Szidat, S., Jenk, T. M., Synal, H.-A., Kalberer, M., Wacker, L., Hajdas, I., Kasper-Giebl, A., and
673 Baltensperger, U.: Contributions of fossil fuel, biomass-burning, and biogenic emissions to
674 carbonaceous aerosols in Zurich as traced by ^{14}C , *J. Geophys. Res.*, 111, D07206, 2006.

675 Szidat, S., Prévôt, A. S. H., Sandradewi, J., Alfarra, M. R., Synal, H. A., Wacker, L., and
676 Baltensperger, U.: Dominant impact of residential wood burning on particulate matter in
677 Alpine valleys during winter, *Geophys. Res. Lett.*, 34, L05820, 2007.

678 Szidat, S.: Sources of Asian haze, *Science*, 323, 470-471, 2009.

679 Szidat, S., Ruff, M., Perron, N., Wacker, L., Synal, H.-A., Hallquist, M., Shannigrahi, A. S., Yttri,
680 K. E., Dye, C., and Simpson, D.: Fossil and non-fossil sources of organic carbon (OC) and
681 elemental carbon (EC) in Goeteborg, Sweden, *Atmos. Chem. Phys.*, 9, 1521-1535, 2009.

682 Szidat, S., Salazar, G. A., Vogel, E., Battaglia, M., Wacker, L., Synal, H.-A., and Türler, A.: ¹⁴C
683 Analysis and Sample Preparation at the New Bern Laboratory for the Analysis of
684 Radiocarbon with AMS (LARA), *Radiocarbon*, 56, 561-566, 2014.

685 Viana, M., Reche, C., Amato, F., Alastuey, A., Querol, X., Moreno, T., Lucarelli, F., Nava, S.,
686 Cazolai, G., Chiari, M., and Rico, M.: Evidence of biomass burning aerosols in the Barcelona
687 urban environment during winter time, *Atmos. Environ.*, 72, 81-88, 2013.

688 Wacker, L., Fahrni, S. M., Hajdas, I., Molnar, M., Synal, H. A., Szidat, S., and Zhang, Y. L.: A
689 versatile gas interface for routine radiocarbon analysis with a gas ion source, *Nucl. Instrum.*
690 *Meth. B*, 294, 315-319, 2013.

691 Weber, R. J., Sullivan, A. P., Peltier, R. E., Russell, A., Yan, B., Zheng, M., de Gouw, J., Warneke,
692 C., Brock, C., Holloway, J. S., Atlas, E. L., and Edgerton, E.: A study of secondary organic
693 aerosol formation in the anthropogenic-influenced southeastern United States, *J. Geophys.*
694 *Res.*, 112, D13302, 2007.

695 Weilenmann, M., Favez, J.-Y., and Alvarez, R.: Cold-start emissions of modern passenger cars at
696 different low ambient temperatures and their evolution over vehicle legislation categories,
697 *Atmos. Environ.*, 43, 2419-2429, 2009.

698 WHO: Air Quality Guidelines: Global Update 2005: Particulate Matter, Ozone, Nitrogen Dioxide
699 and Sulfur Dioxide, World Health Organization, 2006.

700 Yang, F., Tan, J., Zhao, Q., Du, Z., He, K., Ma, Y., Duan, F., Chen, G., and Zhao, Q.:
701 Characteristics of PM_{2.5} speciation in representative megacities and across China, *Atmos.*
702 *Chem. Phys.*, 11, 5207-5219, 2011.

703 Yttri, K. E., Simpson, D., Stenström, K., Puxbaum, H., and Svendby, T.: Source apportionment of
704 the carbonaceous aerosol in Norway-quantitative estimates based on ¹⁴C, thermal-optical and
705 organic tracer analysis, *Atmos. Chem. Phys.*, 11, 9375-9394, 2011.

706 Zhang, Q., Streets, D. G., He, K., and Klimont, Z.: Major components of China's anthropogenic
707 primary particulate emissions, *Environ. Res. Lett.*, 2, 045027, 2007.

708 Zhang, T., Claeys, M., Cachier, H., Dong, S. P., Wang, W., Maenhaut, W., and Liu, X. D.:

709 Identification and estimation of the biomass burning contribution to Beijing aerosol using
710 levoglucosan as a molecular marker, *Atmos. Environ.*, 42, 7013-7021, 2008.

711 Zhang, Y.-L., Li, J., Zhang, G., Zotter, P., Huang, R.-J., Tang, J.-H., Wacker, L., Prévôt, A. S. H.,
712 and Szidat, S.: Radiocarbon-based source apportionment of carbonaceous aerosols at a
713 regional background site on hainan Island, South China, *Environ. Sci. Technol.*, 48, 2651-
714 2659, 2014a.

715 Zhang, Y.-l., Liu, J.-w., Salazar, G. A., Li, J., Zotter, P., Zhang, G., Shen, R.-r., Schäfer, K.,
716 Schnelle-Kreis, J., Prévôt, A. S. H., and Szidat, S.: Micro-scale (μg) radiocarbon analysis of
717 water-soluble organic carbon in aerosol samples, *Atmos. Environ.*, 97, 1-5, 2014b.

718 Zhang, Y. L., Perron, N., Ciobanu, V. G., Zotter, P., Minguillon, M. C., Wacker, L., Prevot, A. S.
719 H., Baltensperger, U., and Szidat, S.: On the isolation of OC and EC and the optimal strategy
720 of radiocarbon-based source apportionment of carbonaceous aerosols, *Atmos. Chem. Phys.*,
721 12, 10841-10856, 2012.

722 Zhang, Y. L., Zotter, P., Perron, N., Prévôt, A. S. H., Wacker, L., and Szidat, S.: Fossil and non-
723 fossil sources of different carbonaceous fractions in fine and coarse particles by radiocarbon
724 measurement, *Radiocarbon*, 55, 1510-1520, 2013.

725 Zhao, P. S., Dong, F., He, D., Zhao, X. J., Zhang, X. L., Zhang, W. Z., Yao, Q., and Liu, H. Y.:
726 Characteristics of concentrations and chemical compositions for PM_{2.5} in the region of
727 Beijing, Tianjin, and Hebei, China, *Atmos. Chem. Phys.*, 13, 4631-4644, 2013.

728 Zhi, G., Chen, Y., Feng, Y., Xiong, S., Li, J., Zhang, G., Sheng, G., and Fu, J.: Emission
729 Characteristics of Carbonaceous Particles from Various Residential Coal-Stoves in China,
730 *Environ. Sci. Technol.*, 42, 3310-3315, 2008.

731 Zotter, P., El-Haddad, I., Zhang, Y., Hayes, P. L., Zhang, X., Lin, Y.-H., Wacker, L., Schnelle-
732 Kreis, J., Abbaszade, G., Zimmermann, R., Surratt, J. D., Weber, R., Jimenez, J. L., Szidat, S.,
733 Baltensperger, U., and Prévôt, A. S. H.: Diurnal cycle of fossil and non-fossil carbon using
734 radiocarbon analyses during CalNex, *J. Geophys. Res.*, 119, 6818-6835, 2014.

735 **Table 1.** Sampling information.

City	City description (population)	Location	Temperature (°C)
Xian (XA) Northern China	The largest city in Guanzhong city cluster (8.6 million)	34.2 N, 108.9 E	-12 – -1
Beijing (BJ) Northern China	Capital of China, developed megacity in Beijing-Tianjin- Hebei city cluster (20.7 million)	39.9 N, 116.4 E	-9 – -1
Shanghai (SH) Southern China	Industrial and commercial megacity in Yangtze Delta Region city cluster (24 million)	31.3 N, 121.5 E	2 – 11
Guangzhou (GZ) Southern China	Industrial and commercial megacity in Pearl River Delta Region city cluster (12.7 million)	23.1 N, 113.4 E	7 – 19

736

737 **Table 2.** Central values with low and high limits of input parameters for source apportionment using
 738 LHS

Parameter	Low	central	high
EC error factor ^a	0.75	^b	1.25
(lev/OC) _{bb}	0.07	0.11	0.20
(EC/OC) _{bb}	0.10	0.22	0.30
(EC/OC) _{pri,cc}	0.32	0.44	0.62
(EC/OC) _{pri,ve}	0.8	^b	2.1
p	0	^b	0.7
f _M (bb)	1.05	1.10	1.15
f _M (nf)	1.03	^b	^c

739 ^a EC values multiplied by given factor.

740 ^b the average of low and high limits is used.

741 ^c f_M(nf) constrained to be < f_M(bb)

742 **Table 3.** Averages and standard deviations of the mass concentrations ($\mu\text{g}/\text{m}^3$) of PM_{2.5}, OC and EC
 743 as well as EC/OC ratios and fractions of modern (f_M) of OC and EC for samples collected on
 744 moderately polluted days (MPD) (n=3 for each city) and heavily polluted days (HPD) (n=3 for each
 745 city) in Xian, Beijing, Shanghai and Guangzhou.

	PM _{2.5}	OC	EC	EC/OC	$f_M(\text{OC})$	$f_M(\text{EC})$
Xian						
MPD	136±27	24.6±6.3	7.2±1.9	0.30±0.07	0.67±0.04	0.25±0.03
HPD	479±25	94.2±6.8	19.8±0.9	0.21±0.02	0.66±0.02	0.24±0.02
HPD/MPD	3.5±0.7	3.8±1.0	2.7±0.7	0.71±0.17	0.99±0.06	0.98±0.16
Beijing						
MPD	85±17	18.0±3.4	4.0±0.2	0.23±0.06	0.49±0.03	0.30±0.02
HPD	266±49	59.2±7.5	7.7±0.9	0.13±0.03	0.40±0.01	0.23±0.02
HPD/MPD	3.1±0.9	3.3±0.8	1.9±0.2	0.57±0.18	0.82±0.06	0.79±0.09
Shanghai						
MPD	59±10	6.2±1.0	1.9±0.1	0.31±0.04	0.55±0.03	0.21±0.02
HPD	131±3	15.6±0.5	4.2±0.3	0.27±0.02	0.54±0.01	0.24±0.04
HPD/MPD	2.2±0.4	2.5±0.4	2.2±0.2	0.87±0.12	0.99±0.06	1.13±0.22
Guangzhou						
MPD	38±14	5.4±2.3	1.6±0.5	0.31±0.04	0.75±0.05	0.48±0.05
HPD	96±6	23.3±2.2	6.1±0.4	0.26±0.01	0.62±0.01	0.22±0.02
HPD/MPD	2.5±1.0	4.3±1.9	3.8±1.1	0.84±0.11	0.83±0.06	0.47±0.06

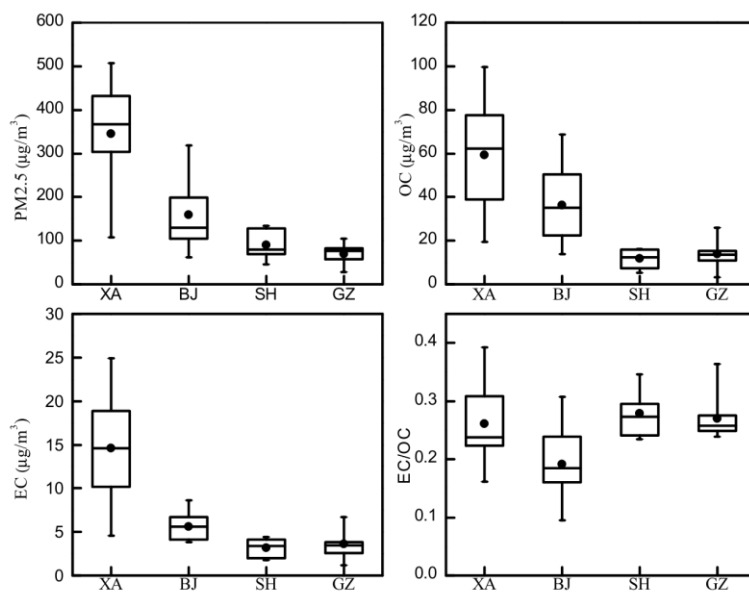
746

747 **Table 4.** Average TC concentration and relative contribution to TC from OC and EC source categories
748 (see in Figure 6) for samples collected in Xian (XA), Beijing (BJ), Shanghai (SH) and Guangzhou
749 (GZ) during the moderately polluted days (MPD) and the heavily polluted days (HPD). Distributions
750 from Latin-hypercube sampling (LHS) are given as medians as well as the 10th and 90th percentiles (in
751 parentheses). See Tab. S2 for an alternative solution for Beijing assuming a higher contribution of coal
752 combustion as explained below in Section 3.3.3.

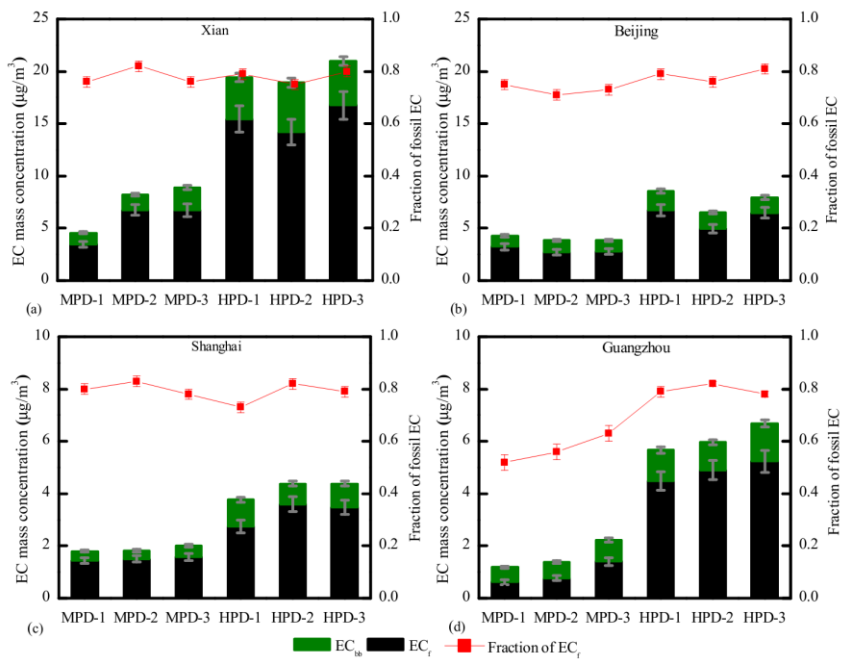
753

Sample code	TC $\mu\text{g}/\text{m}^3$	EC _f %	EC _{bb} %	OC _{pri,f} %	OC _{sec,f} %	OC _{bb} %	OC _{other,nf} %
XA-MPD	31.8	18 (16-19)	5 (4-5)	16 (12-21)	12 (7-16)	25 (19-33)	24 (15-29)
XA-HPD	114.0	14 (12-15)	4 (3-4)	12 (10-16)	19 (15-22)	16 (13-20)	35 (30-38)
BJ-MPD	22.0	13 (12-15)	5 (4-5)	12 (9-16)	32 (27-35)	22 (17-29)	16 (8-20)
BJ-HPD	66.9	9 (8-10)	2 (2-3)	8 (6-11)	47 (44-49)	12 (9-17)	21 (16-23)
SH-MPD	8.1	19 (17-20)	5 (4-5)	17 (13-22)	21 (15-25)	23 (17-31)	16 (7-21)
SH-HPD	19.8	17 (15-18)	5 (4-5)	15 (12-20)	24 (19-28)	19 (15-24)	21 (16-25)
GZ-MPD	7.0	13 (12-15)	10 (9-11)	12 (9-16)	11 (7-14)	45 (37-52)	9 (0-17)
GZ-HPD	29.4	17 (15-18)	4 (4-5)	15 (12-20)	18 (13-22)	20 (16-27)	26 (19-30)

754

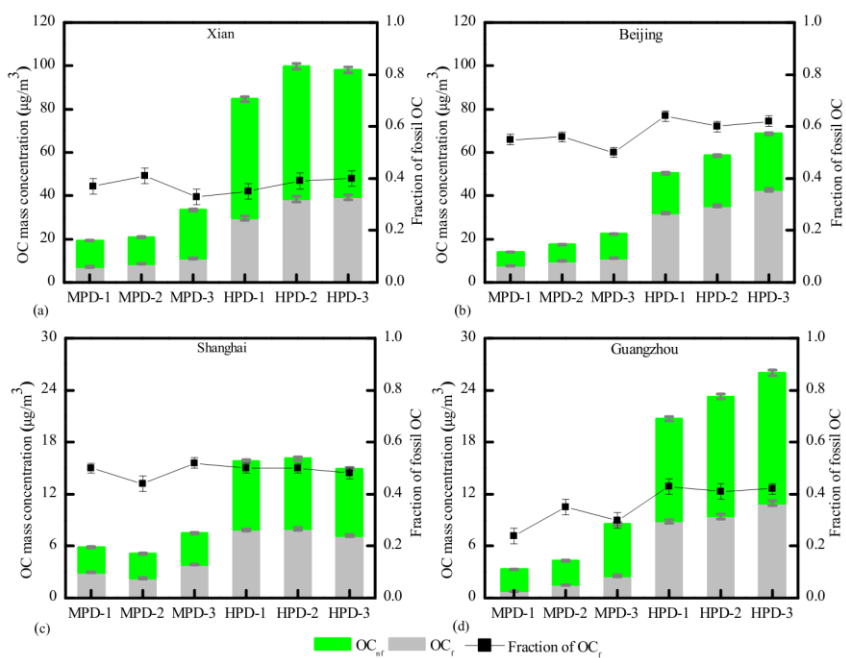


755
 756 **Figure 1.** Whisker-box plots of mass concentrations of PM_{2.5} (a), OC (b) and EC (c) as well as
 757 EC/OC ratios (d) for samples collected in Xian (XA), Beijing (BJ), Shanghai (SH) and Guangzhou
 758 (GZ) during the winter of 2013. The box represents the 25th (lower line), 50th (middle line) and 75th
 759 (top line) percentiles; the solid dots within the box represent the mean values; the end of the vertical
 760 bars represents the 10th (below the box) and 90th (above the box) percentiles.

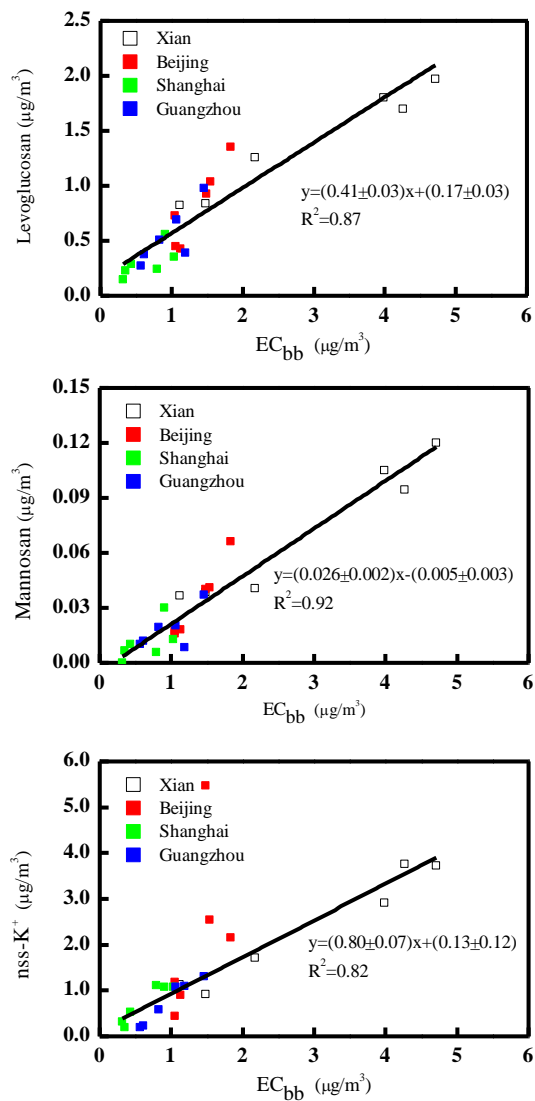


761

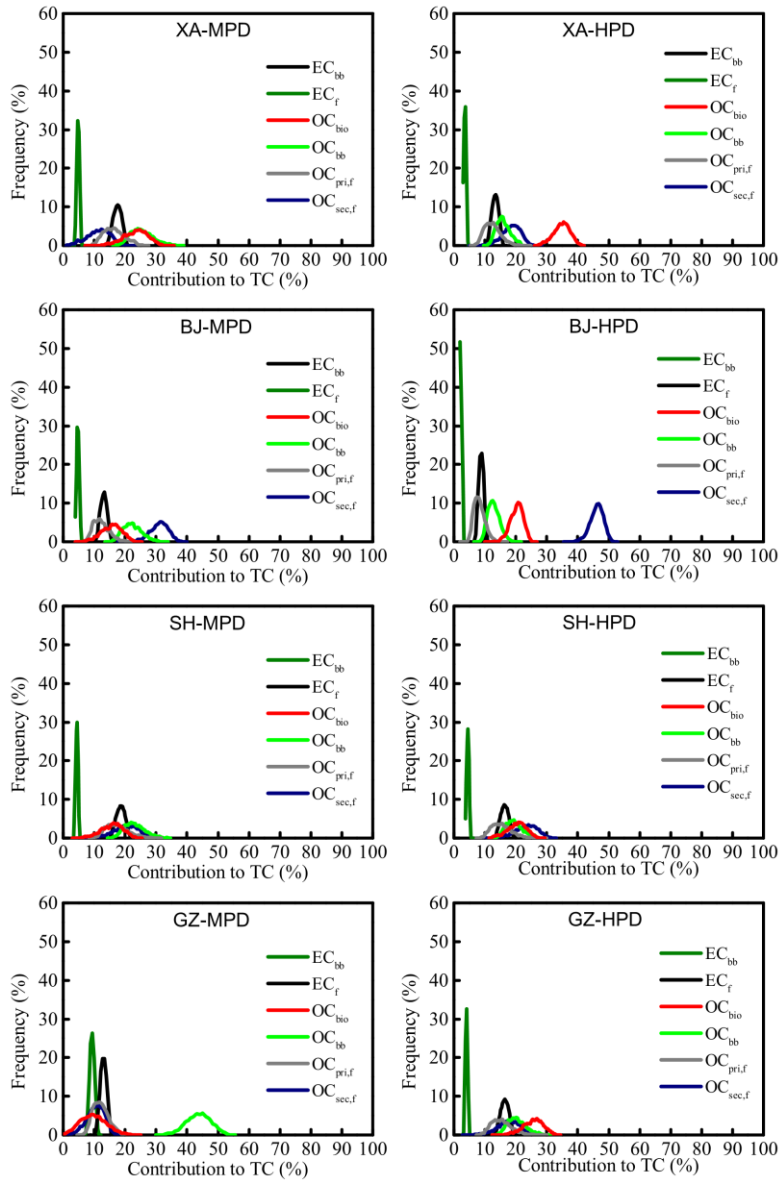
762 **Figure 2.** Mass concentrations ($\mu\text{g}/\text{m}^3$) of EC from biomass burning and fossil-fuel combustion (EC_{bb}
 763 and EC_{fb}, respectively) as well as fractions of fossil EC to total EC for aerosols samples in Xian,
 764 Beijing, Shanghai and Guangzhou during moderately polluted days (MPD) and heavily polluted days
 765 (HPD). Note the different scaling for the northern and the southern cities.

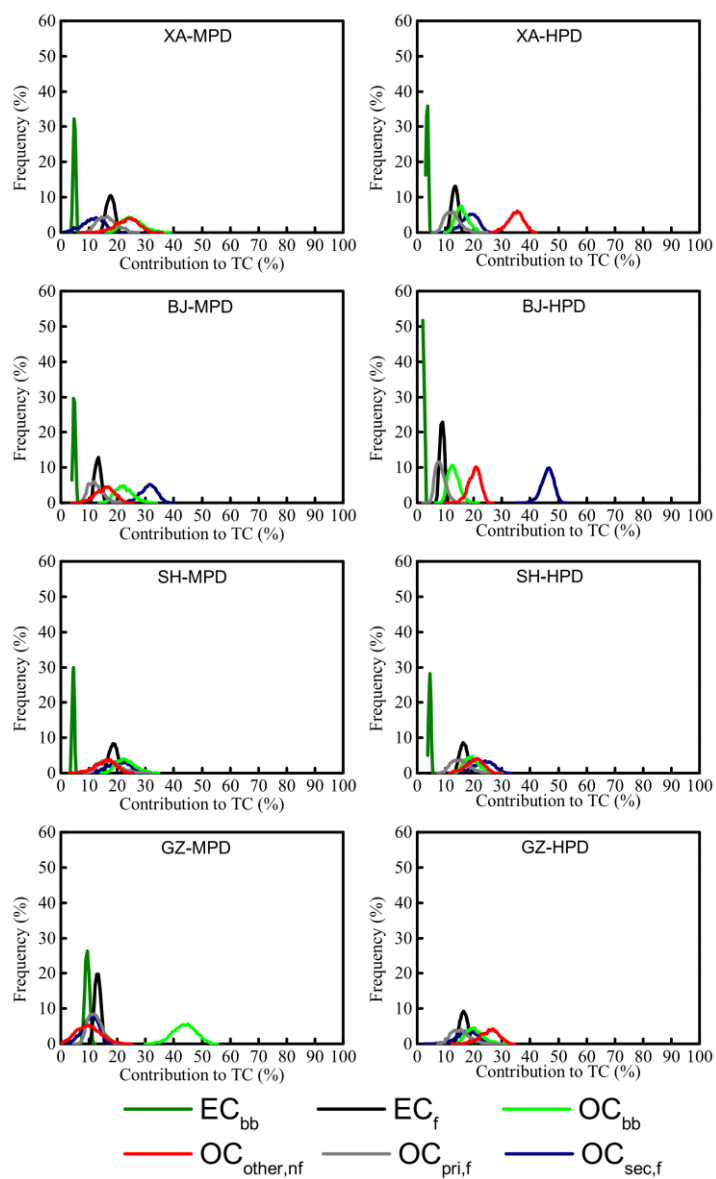


766
 767 **Figure 3.** Mass concentrations ($\mu\text{g}/\text{m}^3$) of OC from non-fossil and fossil emissions (OC_{nf} and OC_{f} ,
 768 respectively) as well as fractions of fossil OC to total OC for samples collected in Xian, Beijing ,
 769 Shanghai and Guangzhou during moderately polluted days (MPD) and heavily polluted days (HPD).
 770 Note the different scaling for the northern and the southern cities.



771
 772 **Figure 4.** Scatter plots of concentrations of EC_{bb} with levoglucosan (top), mannosan (middle) and
 773 non-sea-salt-potassium ($nss-K^+$, bottom).





Formatted: Font: Bold

775

776

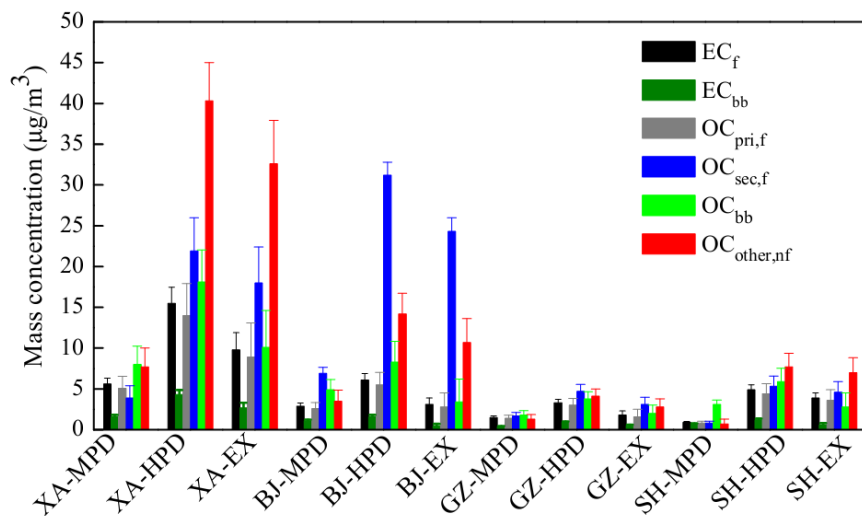
777

778

779

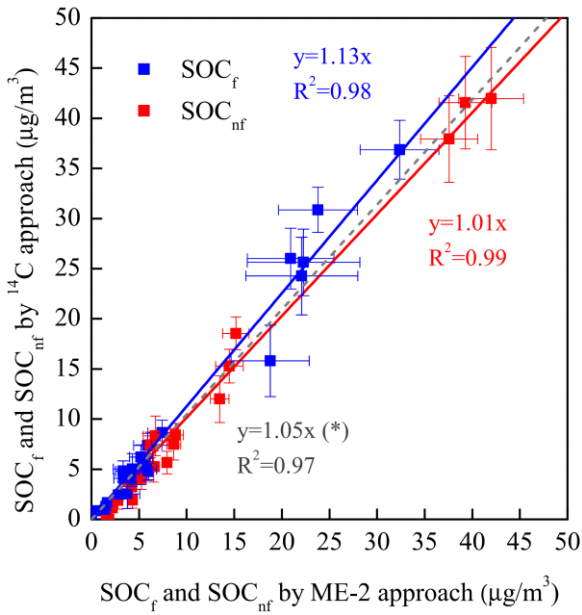
780

Figure 5. Latin-hypercube sampling (LHS) solutions of frequency distributions of the source contributions to TC from OC and EC source categories (see in Table 4) for samples collected in Xian (XA), Beijing (BJ), Shanghai (SH) and Guangzhou (GZ) during the moderately polluted days (MPD) and the heavily polluted days (HPD), respectively.



781

782 **Figure 6.** Average mass concentrations of OC and EC from different sources for samples collected in
 783 Xian (XA), Beijing (BJ), Shanghai (SH) and Guangzhou (GZ) during the moderately polluted days
 784 (MPD), heavily polluted days (HPD) and their corresponding excess (EX=HPD-MPD). Uncertainty
 785 bars represent 10 and 90 percentiles from LHS calculations. See Fig. S1 for an alternative solution for
 786 Beijing assuming a higher contribution of coal combustion as explained [below](#) in Section 3.3.3.



787

788 **Figure 7.** Comparison of secondary OC from fossil and non-fossil sources (i.e. SOC_f and SOC_{nf} ,
 789 respectively) resolved by the ^{14}C and ME-2 approaches. The dashed line denotes a linear
 790 regression fit of SOC_f when excluding data from Beijing yielding an alternative regression slope
 791 marked with an asterisk (*). Note that the intercepts are insignificant for all three cases.